# Research Report

73-2

# ERROR ANALYSIS OF DIGITAL COMMUNICATION BY PAM ON EQUALIZED, BAND RESTRICTED AND INCOHERENT CHANNELS

by

ROBERT MATYAS

Queen's University at Kingston
Department of Electrical Engineering

RESEARCH REPORT NO. 73-2

(2)

# ERROR ANALYSIS OF DIGITAL COMMUNICATION BY PAM ON EQUALIZED, BAND RESTRICTED AND INCOHERENT CHANNELS



by

(1)

Robert Matyas

Department of Electrical Engineering

Queen's University

Kingston, Ontario

Canada

April 1973

## ABSTRACT

The performance of receivers for digital communication by pulse amplitude modulation (PAM) is investigated under specified channel conditions. These channel effects include intersymbol interference, bandpass noise and the addition of a random phase to the carrier. The zero phase receiver examined is the standard baseband receiver for PAM preceded by a product demodulator. The two coherent receivers considered each use a tracking loop in conjunction with the standard receiver. The first receiver incorporates a standard phase-locked loop into the receiver structure while the second utilizes a data-aided carrier tracking loop.

In the case of the zero phase receiver, the system error rate degradation is plotted versus the width of several random phase distributions. Curves indicating the additional signal-to-noise ratio (SNR) required to compensate for these phase distributions are also presented.

The performance of both coherent receivers is examined from the standpoint of system error rate. The theory of the data-aided carrier tracking loop developed by Lindsey and Simon is extended to include the effects of intersymbol interference. The major theoretical result in the study of the data-aided tracking loop is the solution of the Fokker-Planck equation for a first-order tracking loop. This function is then used to average bounds on the demodulator error rate to obtain an estimate of the overall system error rate.

## ACKNOWLEDGEMENTS

This research was supported by the Canadian Federal Department of Communications under DSS Contract OPJ2-0012, the National Research Council of Canada under Grant A7389 and by Bell Canada. In addition, the computing for this research was partially supported by a grant from the School of Graduate Studies at Queen's University. This support is gratefully acknowledged. This report is based on the author's M.Sc. thesis and the guidance of Dr. P.J. McLane in this endeavour is gratefully acknowledged. Discussions held with Dr. P.H. Wittke were also very helpful to the author. Correspondence with Dr. J.K. Cavers of Carleton University, Dr. W.C. Lindsey of the University of Southern California and Dr. M.K. Simon of the Jet Propulsion Laboratory, Passadena, California, is also gratefully acknowledged.

TABLE OF CONTENTS

LIST OF FIGURES

## SUMMARY OF NOTATION

| | |
|---|---|
| $\xi_n$ | a source digit |
| $\xi_\alpha$ | information digit |
| $\hat{\xi}_\alpha$ | unquantized PAM receiver estimate of $\xi_\alpha$ |
| $\hat{\hat{\xi}}_\alpha$ | quantized PAM receiver estimate of $\xi_\alpha$ |
| $\theta$ | random phase introduced into carrier |
| $h(t)$ | channel filter impulse response |
| $h_c(t)$, $h_s(t)$ | quadrature components of $h(t)$ |
| $n(t)$ | a bandpass random process |
| $n_1(t)$, $n_2(t)$ | quadrature components of $n(t)$ |
| $N_o$ | single-sided noise power spectrum height |
| $\sigma^2$ | white noise variance |
| $\psi_i$ | as defined in text |
| $P_L(\theta)$ | conditional Lugannani bound on P(error) |
| $P_{ML}(\theta)$ | conditional modified Lugannani bound on P(error) |
| $P_{L_B}(\theta)$ | conditional lower bound on P(error) |
| $P_{AVG}$ | average of Lugannani and lower bounds |
| $\theta_W$ | phase distribution width |
| $\phi$ | loop phase error |
| $p(\phi)$ | probability density function of $\phi$ |
| $\rho$ | SPLL SNR |
| $B$ | SPLL single-sided bandwidth |

| | |
|---|---|
| $\phi'$ | equalizer single-sided bandwidth |
| (N,K) | as defined in text |

Abbreviations

| | |
|---|---|
| pdf | probability density function |
| P(error) | probability of error |
| SNR | power signal-to-noise ratio |
| LPF | low-pass filter |
| BPF | bandpass filter |
| SPLL | standard phase-locked loop |
| VCO | voltage-controlled oscillator |
| rms | root-mean-squared |

# CHAPTER 1

## INTRODUCTION

For both economic and technical reasons the trend in communication systems is toward information distribution by digital transmission. The design of the communication system is constrained by two fundamental limitations [1]: one technological, the other physical. Efficient system utilization requires minimization of the transmission time. Hence, the objective is to process as much information as possible in the least amount of time. A measure of the signalling speed is the signal's bandwidth - the width of its spectrum. An indication of the system's ability to accommodate the signal is the system's bandwidth. The design of a system must then account for any bandwidth discrepancy that may exist between the processor and the information. This technological consideration is termed the bandwidth limitation. The second constraint is a result of thermal energy that exists in matter and produces undesirable but unavoidable random voltages. These voltages represent the noise limitation.

Yet another disturbance that affects the system

is the uncertainty at the receiver about the exact phase of the received signal. This uncertainty may, for example, develop as a result of slow oscillator drift in the transmitter.

In dealing with discrete information the major criterion of performance is the probability of digit error. The situation to be investigated considers the effect of the disturbances summarized above on the probability of error when a digital pulse-amplitude modulated signal (PAM) is transmitted via a carrier.

1. Research Review

Contamination by broadband noise and distortion caused by the mismatch between system and signal bandwidths, manifested as intersymbol interference, have been examined by Lucky, Salz and Weldon [2] and further studied by George, Coll et al [3] and McLane [4] for the case of a zero phase† receiver and baseband PAM transmission. Lugannani [5] and McLane [4] have derived bounds on the probability of error when the standard equalizer receiver is used. Ho and Spaulding [6] have considered the consequence of phase jitter in the case of a vestigial-sideband amplitude modulation data system (VSB-AM) by using a derived upper bound. Their study uses curves to estimate the accuracy required of a phase jitter recovery system. In the case of large random phase values, the trend has been to incorporate tracking loops into the receiver. The theory of the

† In this report a zero phase receiver is one in which the receiver estimates the value zero for the received phase jitter. A coherent receiver is one in which the incoming phase is continuously estimated.

standard phase-locked loop (SPLL) has been analyzed by several authors, notably Viterbi [7]. Other authors who have documented the SPLL theory are Gardner [8], Lindsey [9] and Stiffler [10]. A recent paper by Lindsey and Simon [11] suggested the use of a data-aided carrier tracking loop which affords a 10 dB improvement in loop signal-to-noise ratio (SNR) over the SPLL when transmission is by phase-shift keying (PSK). However, their study did not include intersymbol interference in discussing loop operation.

## 1.2 Statement of New Results and Outline

The work of Lucky, Salz and Weldon [2] and [3,4,5] on baseband digital PAM is extended to a carrier system. The degradation in system performance when the probability density function (pdf) of the random phase is known is investigated. The improvement in receiver performance when a tracking loop is incorporated into the receiver is discussed for two loop types: the SPLL and the data-aided carrier tracking loop. The work by Lindsey and Simon [11] is modified to include the effect of intersymbol interference caused by the channel and the steady state output phase pdf of this tracking loop is obtained.

While this work examines the case of digital PAM, it is easy to show that the discussion is equally applicable to 2-level PSK digital modulation techniques.

An outline of the work is as follows. Chapter 2 derives an expression for the channel response to a digital PAM input. Chapter 3 considers the degradation in system error rate performance as a function of the phase pdf when a zero phase receiver is used. Chapter 4 investigates the improvement in system reliability when an SPLL is used in conjunction with the standard baseband receiver. Chapter 5 analyzes the data-aided carrier tracking loop as an improved tracking device over the SPLL. Chapter 6 draws conclusions from the study.

# CHAPTER 2

# RESPONSE OF THE BANDPASS CHANNEL TO A PAM INPUT

## 2.1 Introduction

The purpose of this chapter is to analyze the effect of the bandpass channel on the modulated signal. The complete system is first described. This description is then followed by a derivation of the received signal. Once the form of the received signal is known, appropriate receivers may be considered.

## 2.2 System Definition

The communication system considered is depicted in Fig. 1. A binary, memoryless source produces the digit, $\xi_n = \pm 1$, which modulates the real pulse $p(t)$ where $p(t) = 0$ for $t < 0$ and $t > T$. Here $T$ is the bit period. The modulated pulse is multiplied by $\sqrt{2} \cos \omega_c t$ where $\omega_c$ is the carrier frequency. After $N$ digits, the double-sideband suppressed carrier (DSB-SC) transmitter output is

$$x(t) = \sqrt{2} \sum_{n=0}^{N-1} \xi_n \, p(t-nT) \cos \omega_c t$$

which is the input to the channel.

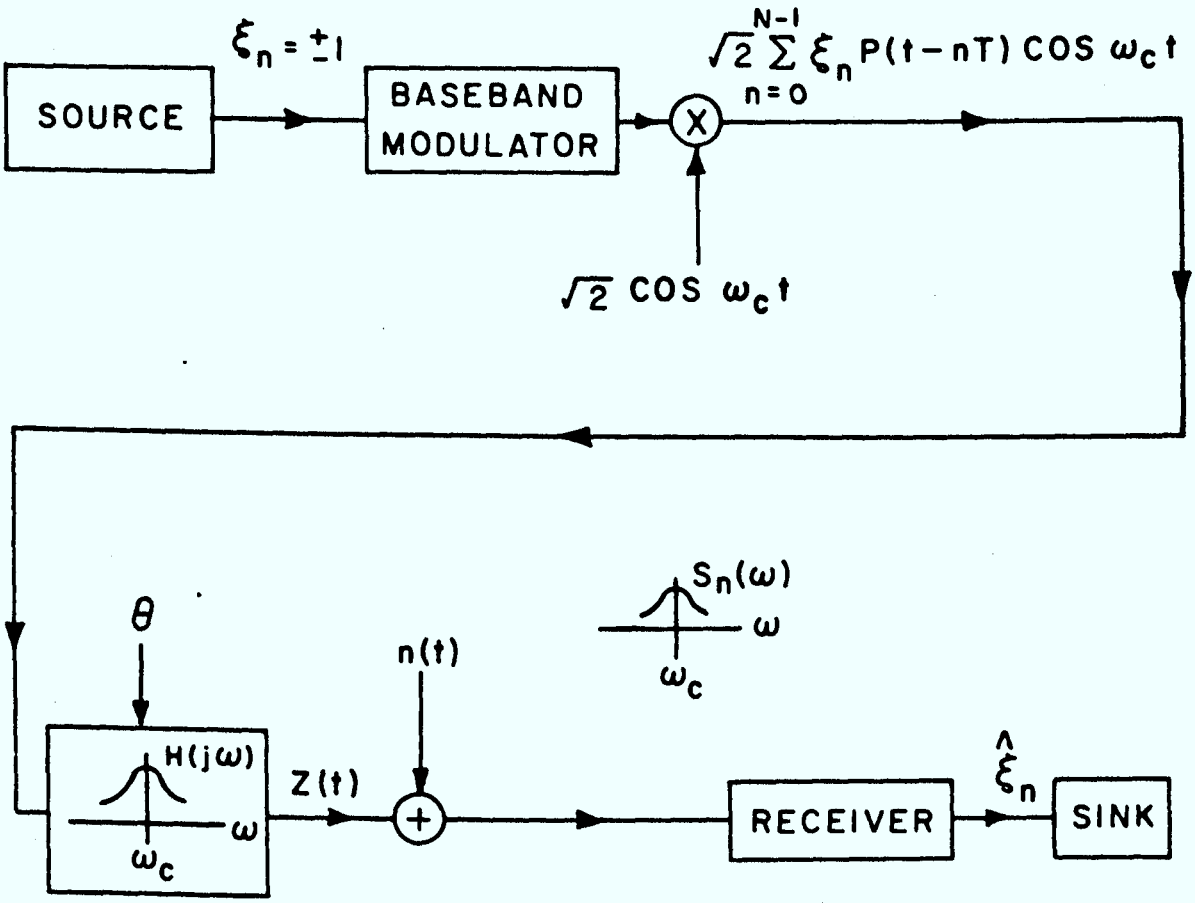


$$Z(t) = \sqrt{2}\sum_{n=0}^{N-1} \xi_n \, g(t-nT) \cos(\omega_c t + \theta)$$

$$g(t) = h_c(t) \circ p(t)$$

FIGURE 1: DIGITAL COMMUNICATION SYSTEM

Characteristic of the channel are the introduction of a random phase into the carrier, distortion of the low-pass portion of the signal via the convolution $h_c(t) \circ p(t)$ and the addition of a bandpass random process n(t) to the distorted signal. Here, $h_c(t)$ is the impulse response of the low-pass portion of the bandpass filter function $H(j\omega)$.

The received signal is demodulated to baseband and then passed through a baseband receiver. The receiver uses a specified decision rule to estimate the information digit. The estimate is then accepted by a data sink.

## 2.3 Channel Model

The channel is modelled by a bandpass filter whose output z(t) is corrupted by additive Gaussian noise. The filter function $H(j\omega)$ is centred about $\omega_c$. The bandpass impulse response may then be represented in terms of two quadrature components. Using the notation of Van Trees [12, p.573] the impulse response, h(t), may be written as

$$h(t) = 2h_c(t) \cos \omega_c t + 2h_s(t) \sin \omega_c t$$

where $h_c(t)$ and $h_s(t)$ are two low-pass functions. A complex impulse response may be defined by letting

$$\tilde{h}(t) \triangleq h_c(t) - j\, h_s(t)$$

Assuming the complex impulse response to be

conjugate symmetric, i.e., $h_s(t) = 0$, implies

$$h(t) = 2h_c(t) \cos \omega_c t$$

Using complex representation, the impulse response may be written as

$$h(t) = \mathrm{Re}[2\tilde{h}(t)\, e^{j\omega_c t}]$$

Similarly, the transmitter output may be written as

$$x(t) = \mathrm{Re}[\sqrt{2} \sum_{n=0}^{N-1} \xi_n\, p(t-nT)\, e^{j\omega_c t}]$$

The channel introduces the random phase $\theta$, with a given probability density function, into the carrier. The steady-state output of the channel filter may then be written as the causal convolution

$$z(t) = \int_0^t h(t-\tau)\, x'(\tau)\, d\tau \qquad (2.3.1)$$

where

$$x'(t) = \mathrm{Re}[\sqrt{2} \sum_{n=0}^{N-1} \xi_n\, p(t-nT)\, e^{j(\omega_c t+\theta)}]$$

[Introducing th phase at this point indicates that the model applies when $\theta$ is due to either transmitter oscillator drift or channel perturbations. The random phase acquired in radio propagation on long haul switched telephone network channels is an example of a channel perturbation.] Substitution of the integrand terms in (2.3.1) gives

$$z(t) = \int_0^t \mathrm{Re}[2\tilde{h}(t-\tau)\, e^{j\omega_c(t-\tau)}] \cdot$$

$$\mathrm{Re}[\sqrt{2} \sum_{n=0}^{N-1} \xi_n\, p(\tau-nT)\, e^{j(\omega_c\tau+\theta)}]\, d\tau \qquad (2.3.2)$$

Using the identity

$$\mathrm{Re}[\alpha] \cdot \mathrm{Re}[\beta] = \frac{1}{2}\mathrm{Re}[\alpha\beta + \alpha\beta^*]$$

(2.3.2) becomes

$$z(t) = \sqrt{2} \sum_{n=0}^{N-1} \xi_n \{\int_0^t \mathrm{Re}[\tilde{h}(t-\tau)\, p(\tau-nT)\, e^{j(\omega_c t+\theta)}$$

$$+ \tilde{h}^*(t-\tau)\, p(\tau-nT)\, e^{j(\omega_c t-\theta)}\, e^{-2j\omega_c\tau}]\, d\tau\} \quad (2.3.3)$$

As $\tilde{h}(t)$ and $p(t)$ are both low-pass, the second term of the integrand in (2.3.3) contributes negligibly. Hence, the filter output is

$$z(t) = \sqrt{2} \sum_{n=0}^{N-1} \xi_n \int_0^t \mathrm{Re}[\tilde{h}(t-\tau)\, p(\tau-nT)\, e^{j(\omega_c t+\theta)}]\, d\tau$$

$$= \sqrt{2} \sum_{n=0}^{N-1} \xi_n\, g(t-nT) \cos(\omega_c t+\theta)$$

where

$$g(t) = \int_0^t h_c(t-\tau)\, p(\tau)\, d\tau$$

$$= h_c(t) \circ p(t)$$

and $\circ$ denotes causal convolution.

The received signal can then be written as

$$y'(t) = z(t) + n(t)$$

$$= \sqrt{2} \sum_{n=0}^{N-1} \xi_n \, g(t-nT) \cos(\omega_c t+\theta) + n(t) \qquad (2.3.4)$$

where n(t) is a Gaussian random process with a two-sided spectral height of $N_o/2$ watts/Hz.

Equation (2.3.4) gives the steady-state channel output. This representation indicates that intersymbol interference, reflected through g(t), exists over the N digit ensemble

$$(\xi_0, \xi_1, \ldots, \xi_\alpha, \ldots, \xi_{N-1})$$

where $\xi_{N-1}$ is the most recent digit transmitted. The information digit is $\xi_\alpha$ and the remaining elements of the ensemble are treated as interference. The subscript $\alpha$ will be defined later.

The more general case of a non-conjugate symmetric channel is treated in Appendix A. This is included for reference for additional work as no theory for random phase compensation for these channels is developed in this thesis.

## 2.4 Summary

The channel response to a digital PAM signal has been derived for a known filter impulse response, a

specified phase pdf and a measured white noise spectral height. The major assumption has been that of a conjugate symmetric channel.

# CHAPTER 3

# THE ZERO PHASE RECEIVER

## 3.1 Introduction

The zero phase receiver is designed on a zero-phase assumption. This means that the receiver structure assumes that the random phase $\theta = 0$.

This chapter assesses the consequences of a small non-zero phase in the PAM carrier upon the performance of a zero phase receiver. The performance is measured through the probability of digit error. In the case of a PAM receiver the expression for the probability of error is computationally formidable. As a result, error bounds are applied which confine the error probability within a neighbourhood of the true value.

In essence, McLane's [4] work on upper and lower bounds for the probability of digit error for data transmission by PAM is extended to include the case of phase jitter, $\theta$. These bounds will merely be quoted in this work as the format in [4] is quite tutorial. Further, the range of $\theta$ for which these bounds presently apply is extended to $[-\pi, \pi]$ from $[-\pi/2, \pi/2]$.

## 3.2 Receiver Structure

The receiver comprises two units: a baseband demodulator and a baseband receiver. The demodulator is a product demodulator as shown in Fig. 2. The output, $y(t)$, of this receiver segment is given by

$$y(t) = \sqrt{2} \cos \omega_c t \cdot y'(t) \tag{3.2.1}$$

which when (2.3.4) is substituted for $y'(t)$ becomes

$$y(t) = \sqrt{2} \cos \omega_c t \{\sqrt{2} \sum_{n=0}^{N-1} \xi_n g(t-nT) \cdot \cos (\omega_c t+\theta) + n(t)\} \tag{3.2.2}$$

Using the trigonometric identity

$$2 \cos A \cos B = \cos (A+B) + \cos (A-B) \tag{3.2.3}$$

(3.2.2) can be written as

$$y(t) = \sum_{n=0}^{N-1} \xi_n g(t-nT) [\cos (2\omega_c t+\theta) + \cos \theta] + \sqrt{2} \cos \omega_c t \cdot n(t) \tag{3.2.4}$$

It is convenient to use the decomposition of $n(t)$ given in [11]:

$$n(t) = \sqrt{2}[n_1(t) \cos \omega_c t - n_2(t) \sin \omega_c t] \tag{3.2.5}$$

where $n_1(t)$ and $n_2(t)$ are independent Gaussian random processes with double-sided spectral densities $N_o/2$

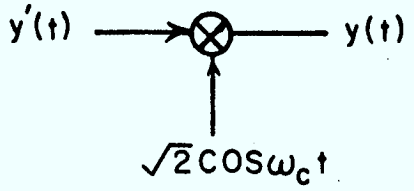


FIGURE 2: PRODUCT DEMODULATOR

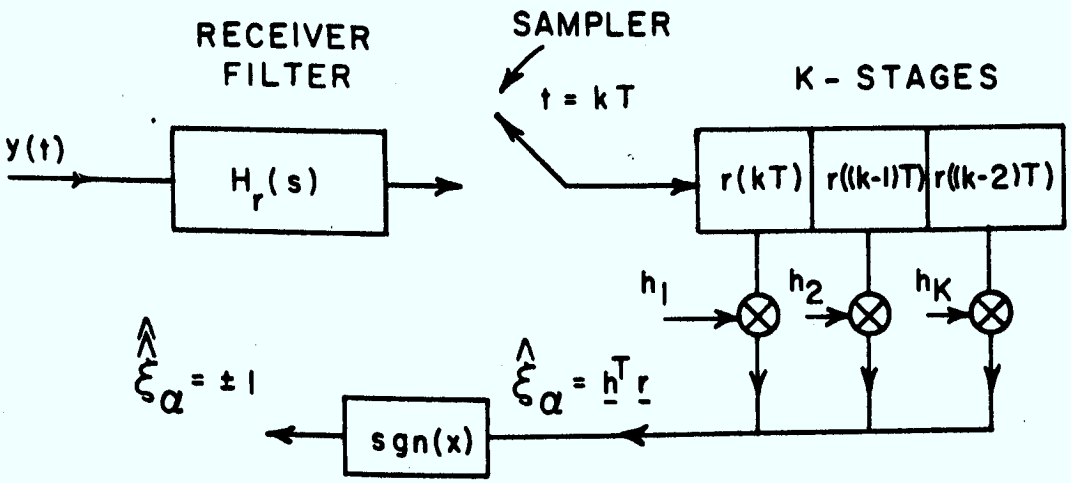


FIGURE 3: A DIGITAL PAM RECEIVER

watts/Hz. Substitution of (3.2.5) in (3.2.4) gives

$$y(t) = \sum_{n=0}^{N-1} \xi_n \, g(t-nT) \, [\cos (2\omega_c t+\theta) + \cos \theta]$$

$$+ 2\cos \omega_c t \, [n_1(t) \cos \omega_c t - n_2(t) \sin \omega_c t] \qquad (3.2.6)$$

Using the identity

$$2 \cos A \sin B = \sin (A+B) - \sin (A-B)$$

and (3.2.3), the second term in (3.2.6) can be expanded to give

$$2 \cos \omega_c t \, [n_1(t) \cos \omega_c t - n_2(t) \sin \omega_c t]$$

$$= n_1(t) \, [\cos 2\omega_c t+1] - n_2(t) \sin 2\omega_c t \qquad (3.2.7)$$

In practice, the product demodulation is accomplished by a device unable to respond to the double-frequency terms present in $y'(t)$ [9,p.74]. Hence, (3.2.6) becomes

$$y(t) = \sum_{n=0}^{N-1} \xi_n \, g(t-nT) \cos \theta + n_1(t) \qquad (3.2.8)$$

The standard receiver for digital PAM [4] is shown in Fig. 3. This baseband receiver consists of a cascade of a low-pass filter, a sampler and a tapped delay line whose outputs, $r_i = r\,[(K-i+1)T]$, are

weighted according to a specified statistical criterion. The contents of the $i^{th}$ stage of the tapped delay line is the receiver filter output sample taken at $t = (K-i+1)T$ where K is the number of delay line stages. The low-pass filter, $H_r(s)$, reduces the effect of broadband noise without significantly distorting the modulation. The tapped delay line with fixed output taps, $h_i$, and summing junction comprise the fixed transversal equalizer [2,p.130]. The equalizer output, $\hat{\xi}_\alpha$, is quantized to give the binary result

$$\hat{\hat{\xi}}_\alpha = \text{sgn}\ (\hat{\xi}_\alpha) \tag{3.2.9}$$

where

$$\text{sgn}(x) = \begin{cases} 1 & x \geq 0 \\ -1 & x < 0 \end{cases}$$

In determining the estimate, the receiver uses K digits where $K \leq N$. In addition, the sampler is assumed synchronized with the digit frame.

For $\theta = 0$, [4] and [13] have shown that the output sample of the K-stage transversal equalizer corresponding to the $\alpha$ digit can be written as

$$\hat{\xi}_\alpha = d + \xi_\alpha\, \psi_{\alpha+1} + \gamma \tag{3.2.10}$$

where

$$d = \sum_{\substack{i=0 \\ i \neq \alpha}}^{N-1} \xi_i \, \psi_{i+1}$$

represents the contribution of the interfering digits, $\gamma$ is the term reflecting filtered white noise and $\xi_\alpha \, \psi_{\alpha+1}$ is the information component. The weighting factor $\psi_i$ is the overall sampled impulse response of the channel-equalizer configuration.

When $\theta \neq 0$ and constant for many digit intervals, a similar expression is obtained for $\hat{\xi}_\alpha$ by defining a new input symbol $\xi_n' = \cos \theta \cdot \xi_n$ in (3.2.8). It will be convenient to associate $\cos \theta$ with the weighting factor $\psi_i$ in the final result. The equalizer output for non-zero phase is then

$$\hat{\xi}_\alpha = d' + \xi_\alpha \, \psi'_{\alpha+1} + \gamma \qquad (3.2.11)$$

where

$$d' = \sum_{\substack{i=0 \\ i \neq \alpha}}^{N-1} \xi_i \, \psi'_{i+1} \qquad (3.2.12)$$

and $\psi_i' = \cos \theta \cdot \psi_i$ with $\psi_i$ being the zero-phase weighting factor. The filtered white noise term, $\gamma$, has a normal pdf characterized by $\eta(o, \sigma^2)$ where $\sigma^2$ is the variance of the filtered version of $n_1(t)$.

## 3.3 Probability of Error

The receiver decision rule is governed by (3.2.9). As a consequence of (3.2.9), (3.2.11) can be used to define the two mutually exclusive error-causing events:

$$A_1 = \{\xi_\alpha = 1\} \cap [d' + \gamma < -\psi'_{\alpha+1}\}$$

$$A_2 = \{\xi_\alpha = -1\} \cap \{d' + \gamma \geq \psi'_{\alpha+1}\}$$

As

$$P[\xi_\alpha = 1] = P[\xi_\alpha = -1] = \frac{1}{2} ,$$

$$P(\text{error}) = \frac{1}{2} [P(d' + \gamma < -\psi'_{\alpha+1}) + P(d' + \gamma \geq \psi'_{\alpha+1})] \qquad (3.3.1)$$

In this work it will be assumed that [4]

$$\psi_{\alpha+1} > 0 \qquad (3.3.2)$$

Substituting $\psi'_i$ for $\psi_i$ in the expansion of (3.3.1) by [4] gives the error probability conditioned on $\theta$:

$$P(\text{error}) = P(d' + \gamma \geq \psi'_{\alpha+1})$$

$$= \frac{1}{2^{N-1}} \sum_{d'_i} \text{erfc} \left(\frac{\psi'_{\alpha+1} + d'}{\sigma}\right) \qquad (3.3.3)$$

In (3.3.3) $d'_i$ corresponds to the $i^{th}$ choice of signs for the $\xi_i$ in (3.2.12) and

$$\text{erfc}(x) = \frac{1}{\sqrt{2\pi}} \int_x^\infty \exp(-\frac{t^2}{2})\, dt \qquad (3.3.4)$$

In (3.3.3) two separate cases can be identified: (1) $0 \leq |\theta| \leq \pi/2$, and (2) $\pi/2 < |\theta| < \pi$. If condition (1) applies then $\cos\theta \geq 0$ and

$$\frac{\psi'_{\alpha+1} + d'}{\sigma} \geq 0$$

However, if condition (2) holds then it will be convenient to let $|\theta| = \pi/2 + v$, where $0 < v < \pi/2$. As a result

$$\frac{\psi'_{\alpha+1} + d'}{\sigma} = \frac{-\sin v}{\sigma} (\psi_{\alpha+1} + d)$$

where

$$\frac{\sin v}{\sigma} (\psi_{\alpha+1} + d) \geq 0$$

The function erfc(x) is symmetric about x = 0. Hence,

$$\text{erfc}(-x) = 1 - \text{erfc}(x) \qquad (3.3.5)$$

Using the result of (3.3.5) in (3.3.3) gives the conditional error probability for condition (2) as

$$P(\text{error}) = 1 - \frac{1}{2^{N-1}} \sum_{d_i} \text{erfc}\ [\frac{\sin v}{\sigma} (\psi_{\alpha+1} + d)]$$

$$= 1 - \frac{1}{2^{N-1}} \sum_{d''_i} \text{erfc}\ (\frac{\psi''_{\alpha+1} + d''}{\sigma}) \qquad (3.3.6)$$

where

$$\psi''_{\alpha+1} = \sin v \cdot \psi_{\alpha+1} \ , \quad d'' = \sum_{\substack{i=0 \\ i\neq\alpha}}^{N-1} \xi_i \, \psi''_{i+1}$$

and $\psi''_i = \sin v \cdot \psi_i$. The term $d''_i$ denotes the $i^{th}$ choice of signs for the $\xi_i$ in d".

## 3.4 Bounds on P(error)

The summations in (3.3.6) and (3.3.3) are of a common form. Bounds on the probability of digit error in (3.3.3) when $\theta = 0$ have been derived in [4]. The substitution of $\psi'_i$ for $\psi_i$ in the expressions for these bounds produces the following phase-conditioned results.

### Upper Bound

The upper bound makes use of the Chernoff inequality and a formula derived by Lugannani [5]:

$$\begin{aligned} P(\text{error}) \leq 1 &- \tfrac{1}{2}\,\Phi(\eta - m'\beta(1-\beta^2)^{-\frac{1}{2}}) - \tfrac{1}{2}\,\Phi(\eta + m'\beta(1-\beta^2)^{-\frac{1}{2}}) \\ &+ \beta \exp(-\tfrac{\eta^2}{2}(1-\beta^2)) \cdot \{\Phi(\sqrt{\ln 4}\,(1-\beta^2)^{-\frac{1}{2}} + \eta\beta) \\ &- \Phi(\sqrt{\ln 4}\,(1-\beta^2)^{-\frac{1}{2}} - \eta\beta) + \Phi(M(1-\beta^2)^{-\frac{1}{2}} - \eta\beta) \\ &- \Phi(M(1-\beta^2)^{-\frac{1}{2}} + \eta\beta)\} \end{aligned} \qquad (3.4.1)$$

where

$$M = \max [\bar{B}, \sqrt{\ln 4}], \quad m' = \min [\bar{B}, \sqrt{\ln 4}],$$

$$\bar{B} = \frac{d^i_{max}}{\sigma_d} = \frac{1}{\sigma_d} \sum_{\substack{i=1 \\ i \neq \alpha+1}}^{N} |\psi_i'| \quad ,$$

$$\sigma_d^2 = \sum_{\substack{i=1 \\ i \neq \alpha+1}}^{N} (\psi_i')^2 \quad , \quad \eta = \frac{\psi'_{\alpha+1}}{\sigma} \quad ,$$

$$\beta^2 = \frac{\sigma_d^2}{\sigma^2 + \sigma_d^2} \quad ,$$

$$\Phi(x) = \frac{1}{\sqrt{2\pi}} \int_{-\infty}^{x} \exp(-\frac{t^2}{2})\, dt$$

Note that $d^i_{max}$ is the largest value of $d^i$ obtainable from (3.2.12). This expression will be termed the Lugannani bound and denoted by $P_L(\theta)$ where the argument $\theta$ indicates the conditional nature of the bound.

Modified Upper Bound

A simplification [4] of (3.4.1) gives

$$P(\text{error}) \leq 1 - \Phi(\eta) + \beta \exp(-\frac{\eta^2}{2}(1-\beta^2)) \cdot$$

$$\{2\,\Phi(\eta\beta) - \Phi(\bar{B}(1-\beta^2)^{-\frac{1}{2}} + \eta\beta)$$

$$- \Phi(\eta\beta - \bar{B}(1-\beta^2)^{-\frac{1}{2}})\} \qquad (3.4.2)$$

Equation (3.4.2) will be called the modified Lugannani bound and represented by $P_{ML}(\theta)$.

Lower Bound

A lower bound based on Jensen's inequality is derived in [4] and is given by

$$P(\text{error}) \geq \text{erfc}\ \left(\frac{\psi'_{\alpha+1}}{\sigma}\right) \qquad (3.4.3)$$

This lower bound will be represented by $P_{LB}(\theta)$.

The bounds above are applicable when the condition of (3.3.2) holds and $0 \leq |\theta| \leq \pi/2$. When $\pi/2 < |\theta| < \pi$, then (3.4.1), (3.4.2) and (3.4.3) may be used to bound the second term in (3.3.6). However, $\psi'_i$ must be replaced by $\psi''_i$ in these bounds. In general, $P_L(\theta)$, $P_{ML}(\theta)$ and $P_{LB}(\theta)$ will refer to either (3.3.3) or the second term of (3.3.6) depending on the value of $\theta$ considered.

The nature of (3.3.6) indicates that the lower bound can be used to give an upper bound on P(error). This can be shown by letting W represent the second term of (3.3.6). Then,

$$P_{LB}(\theta) \leq W$$

where

$$P(\text{error}) = 1 - W$$

As a result

$$P(\text{error}) \leq 1 - P_{LB}(\theta)$$

Similarly, the upper bounds prescribe lower bounds on P(error).

## 3.5 Example 1 Parameters

The receiver considered here consists of a five-stage tapped delay line whose output taps are determined by the minimum mean-square estimation error criterion:

$$E[(\xi_\alpha - \hat{\xi}_\alpha)^2] = \min \tag{3.5.1}$$

where $E[\cdot]$ denotes the expected value operator. For convenience (3.2.8) is repeated:

$$y(t) = \sum_{n=0}^{N-1} \xi_n \, g(t-nT) \cos\theta + n_1(t) \tag{3.5.2}$$

where

$$g(t) = h_c(t) \circ p(t)$$

The form of (3.5.2) indicates that intersymbol interference is assumed to exist over the N-digit ensemble. In describing a particular ensemble and receiver delay line structure, the notation (N,K) will be used. Hence, (7,5) implies a 7-digit ensemble with the receiver having a five-stage delay line.

The situation investigated by McLane [4] will be extended to account for carrier phase uncertainty. Specifically,

$$H(s) = \frac{a}{s+a} \qquad \underline{\text{channel filter}} \qquad (3.5.3)$$

$$h_c(t) = a\, e^{-at}$$

$$H_r(s) = \frac{\phi'}{s+\phi'} \qquad \underline{\text{receiver filter}} \qquad (3.5.4)$$

$$h_r(t) = \phi' e^{-\phi' t}$$

$$g(t) = \begin{cases} b(1-e^{-at}) & 0 \le t \le T \\ b(1-e^{-\beta})e^{-a(t-T)} & t \ge T \end{cases} \qquad (3.5.5)$$

where b is the height of p(t) with p(t) a rectangular pulse, T is the digit duration and $\beta = aT$. It will be assumed that a = 1, b = 1 and T = 1. The receiver and channel filter bandwidths are related by $\lambda^{-1} = \phi'/a$.

The detected SNR will be as in [4]

$$\text{SNR} \triangleq 10 \log_{10} \frac{2b^2}{N_o \phi'} \qquad (3.5.6)$$

where $b^2$ is the power in p(t) and $\phi'$ is the single-sided LPF bandwidth.

## 3.6 Bounds Averaged Over the Phase Pdf

The upper and lower bounds quoted in Sec. 3.4 are all conditioned on the random phase $\theta$. The bounds may be integrated numerically over the phase pdf:

$$P_G = \int_{-\pi}^{\pi} P_G(\theta) \cdot p(\theta)\, d\theta$$

$$= 2 \int_{0}^{\pi} P_G(\theta) \cdot p(\theta)\, d\theta \qquad (3.6.1)$$

where $P_G$ is the general expression representing an averaged bound, $P_G(\theta)$ is the conditional probability and $p(\theta)$ is the specified phase pdf. Both $P_G(\theta)$ and $p(\theta)$ are symmetric about $\theta = 0$. Provided the values of $P_L$ and $P_{LB}$ determined by (3.6.1) are within an order-of-magnitude, their arithmetic mean, $P_{AVG}$, may be used as an estimate of the probability of digit error.

## 3.7 Performance Curves - Example 1

Figures 4-7 are concerned with the (7,5) case. McLane [4] has found that the $\psi_i$ when the SNR = 19 dB are given by:

$$\begin{bmatrix} \psi_1 \\ \psi_2 \\ \psi_3 \\ \psi_4 \\ \psi_5 \\ \psi_6 \\ \psi_7 \end{bmatrix} = \begin{bmatrix} .95E\text{-}02 \\ .26E\text{-}01 \\ -.22E\text{-}01 \\ .24E\text{-}01 \\ .96E\ 00 \\ .20E\text{-}01 \\ -.49E\text{-}02 \end{bmatrix}$$

where $\psi_{\alpha+1} = \psi_5$ and $\alpha = (K-1/2) + L$ with $L = N-K$. The value of $\sigma$ corresponding to SNR = 19 dB is .188.

Figure 4 is a plot of the bounds $P_L$, $P_{ML}$ and $P_{LB}$ as a function of the phase pdf width. The density functions considered are uniform on the interval $[-\theta_o, \theta_o]$.

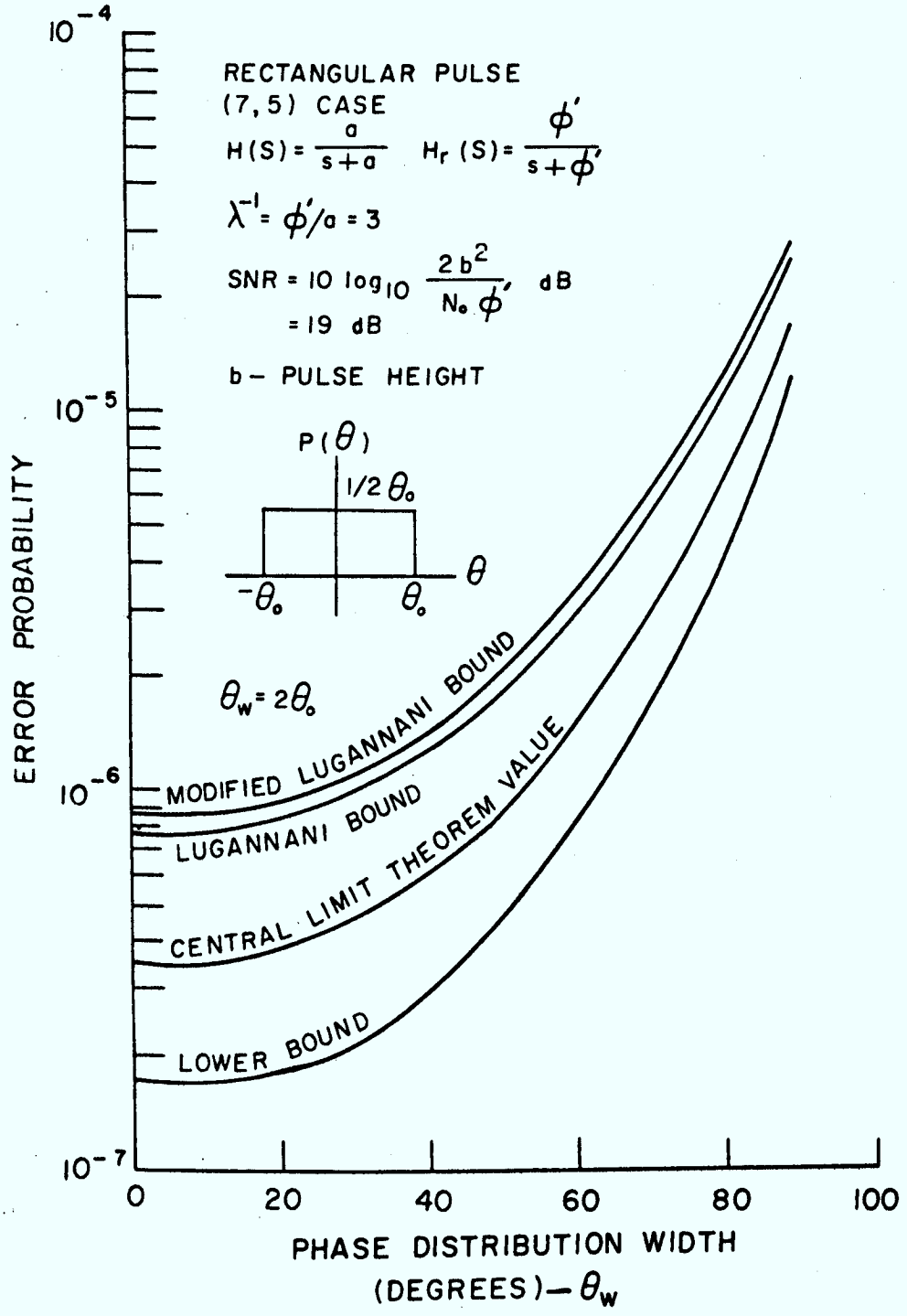


FIGURE 4: SYSTEM ERROR RATE DEGRADATION VERSUS UNIFORM PHASE DISTRIBUTION WIDTH - (7, 5) CASE

The ordinate intercepts are the zero-phase values, i.e., the operating P(error) bounds predicted by the baseband receiver with no phase uncertainty. The Lugannani and lower bounds differ by at most a factor of 4 and consequently $P_{AVG}$ gives a reasonable estimate of P(error). The curve marked, "Central Limit Theorem Value", is based on assuming d' in (3.3.3) to have a normal pdf. The result is included for comparison only as the assumption about d' is not valid. Fig. 5. is a plot of the $P_{AVG}$ corresponding to the results of Fig. 4. The $P_{AVG}$ curve indicates that uniform distribution widths as great as 70° are tolerable before an order-of-magnitude error rate degradation occurs. Figures 6 and 7 portray similar conditions except that the pdf characteristic is changed. The pdf used is a truncated version of the density given by Van Trees [14, p. 158]

$$p'(\theta) = \frac{\exp(\alpha \cos \theta)}{2\pi I_o(\alpha)} \qquad (3.7.1)$$

where $I_o(\alpha)$ is the modified Bessel function of zero-order and argument $\alpha$ where $\alpha$ is a parameter. Incidentally, the pdf of (3.7.1) is the steady-state output phase density of a first order phase-locked loop which will be treated in Chap. 4. For the non-uniform phase distribution, Fig. 7 indicates that a maximum density of approximately 80° is acceptable before the error rate degrades by one order-of-magnitude.

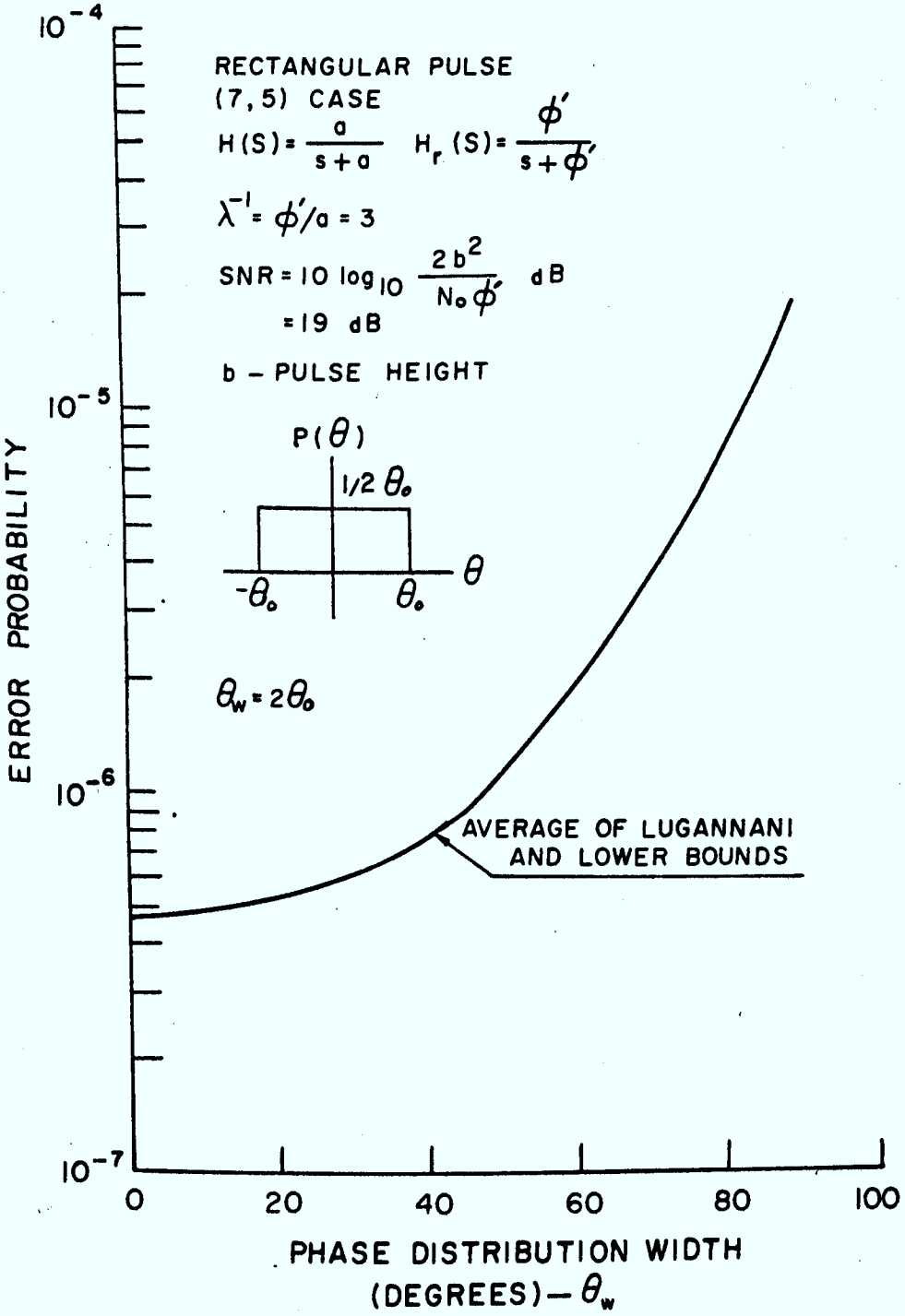


FIGURE 5: SYSTEM ERROR RATE DEGRADATION VERSUS UNIFORM PHASE DISTRIBUTION WIDTH - (7,5) CASE

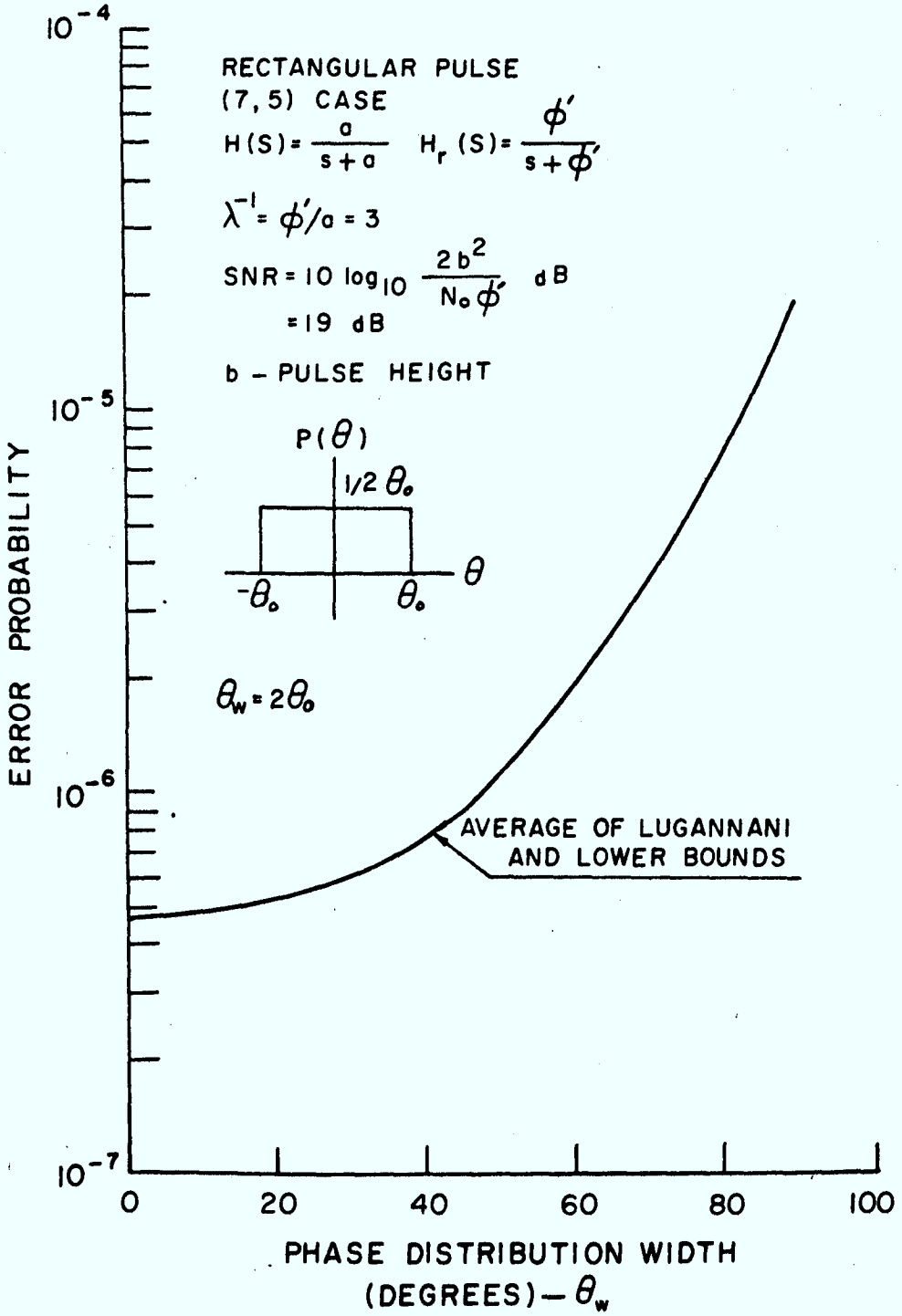


FIGURE 5: SYSTEM ERROR RATE DEGRADATION VERSUS UNIFORM PHASE DISTRIBUTION WIDTH - (7,5) CASE

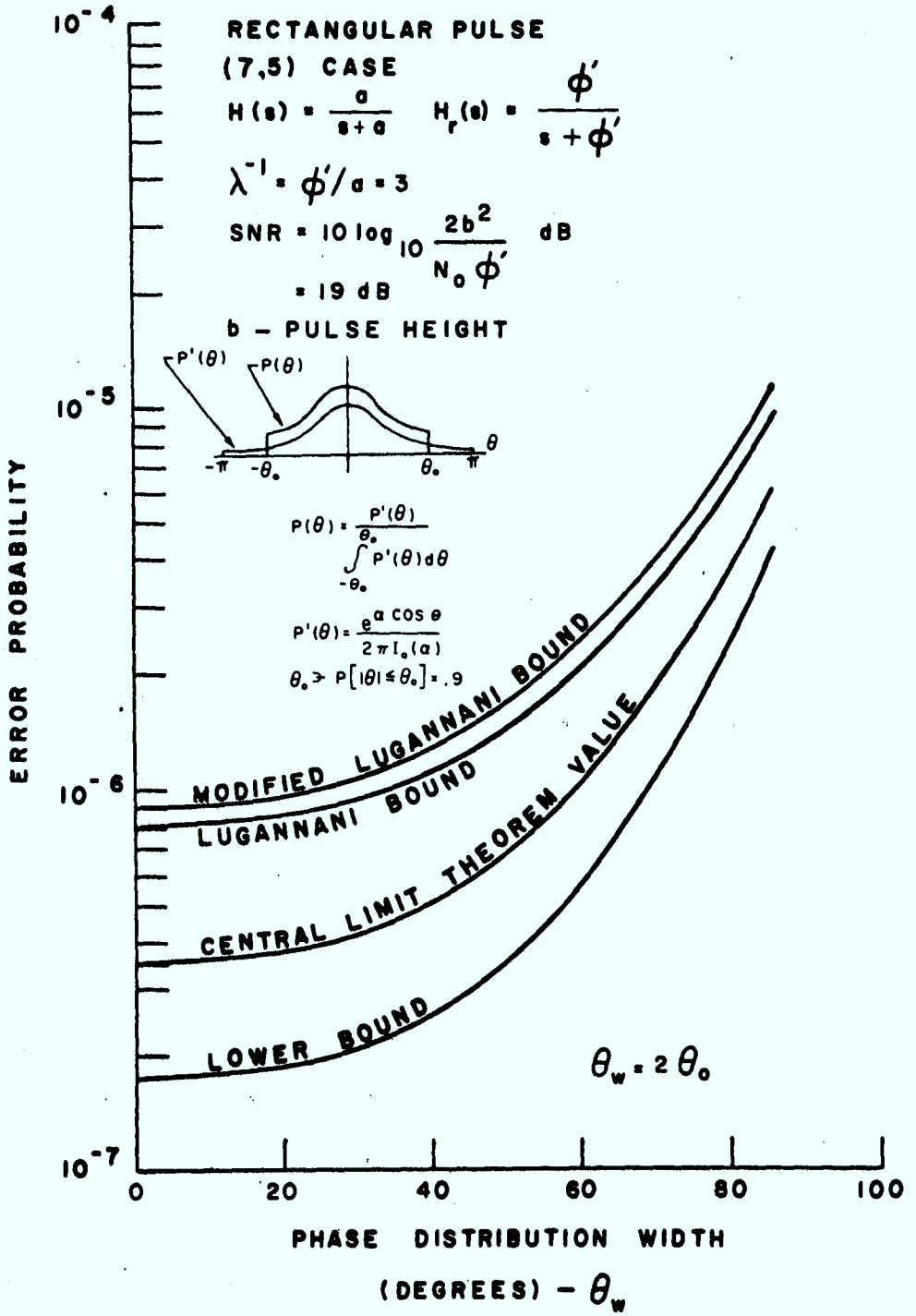


FIGURE 6: SYSTEM ERROR RATE DEGRADATION VERSUS NON-UNIFORM PHASE DISTRIBUTION WIDTH - (7,5) CASE

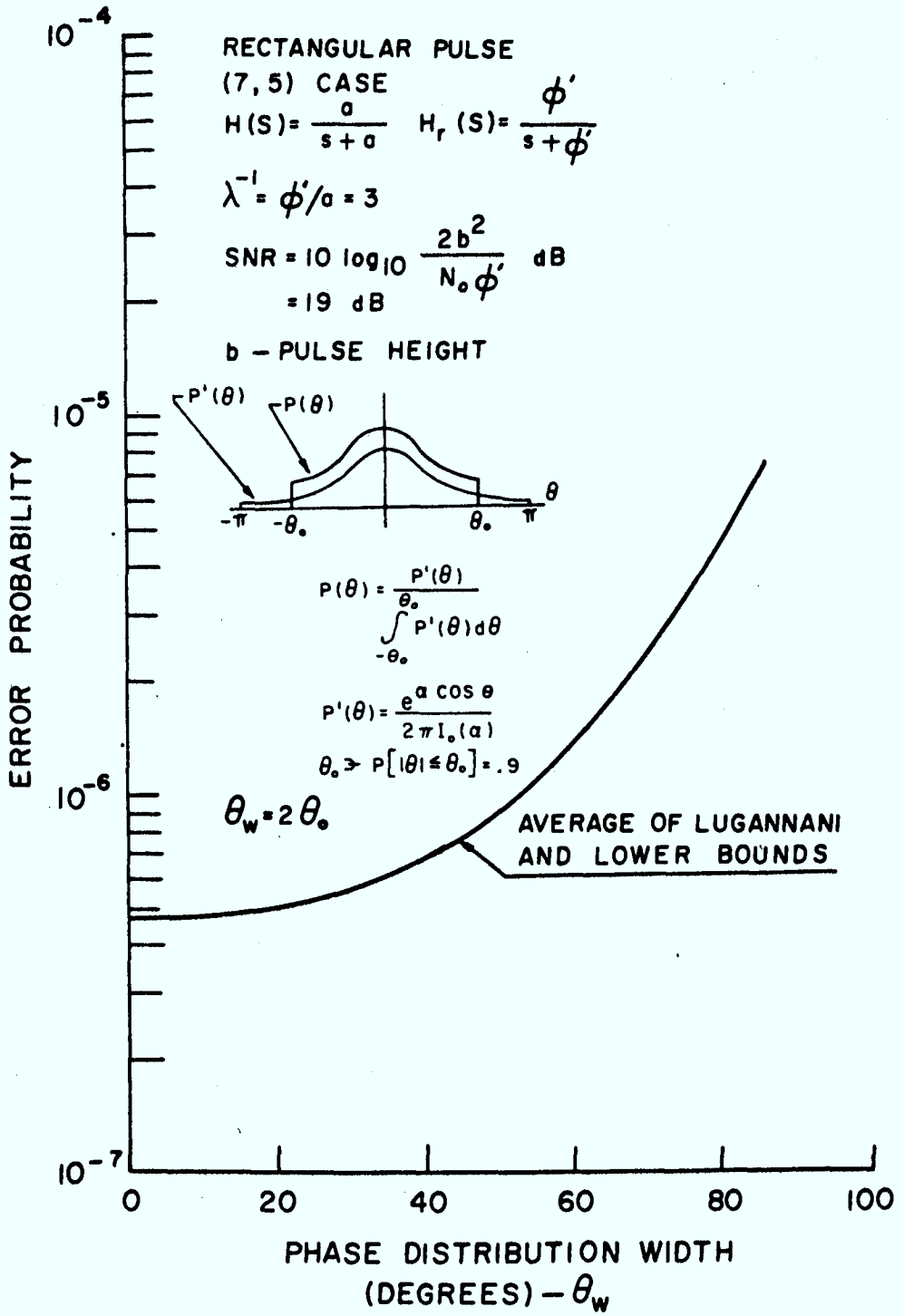


FIGURE 7: SYSTEM ERROR RATE DEGRADATION VERSUS NON-UNIFORM PHASE DISTRIBUTION WIDTH - (7, 5) CASE

The error bounds of Figs. 4-7 considered inter-symbol interference to exist over N = 7 digits. Figs. 8-11 indicate that when N is increased to 9 the P(error) remains at nearly the same level as that of the (7,5) situation.

## 3.8 Phase Compensation by SNR Adjustment

The expansion of (3.2.11) gives

$$\hat{\xi}_\alpha = d \cos \theta + \xi_\alpha \psi_{\alpha+1} \cos \theta + \gamma \qquad (3.8.1)$$

As $\theta$ increases from 0 to $\pi/2$, the information to filtered white noise ratio given by

$$\text{INR} \triangleq \frac{(\psi_{\alpha+1} \cos \theta)^2}{\sigma^2} \qquad (3.8.2)$$

decreases. To compensate for this phase degradation, the received signal SNR can be increased. The following two schemes describe the SNR adjustment methodology.

### Iterative Method

The filtered white noise term $\gamma$ is a function of the white noise spectral height and consequently of the SNR by (3.5.6). Hence, a given receiver structure and detected SNR determine $\sigma^2$. Both $P_L$ and $P_{LB}$ are functions of $\sigma^2$. Provided that $P_L$ and $P_{LB}$ are within an order of magnitude, $P_{AVG}$ represents a reasonable estimate of P(error). This means $P_{AVG}$ is a function of $\sigma^2$ as well as of the phase pdf.

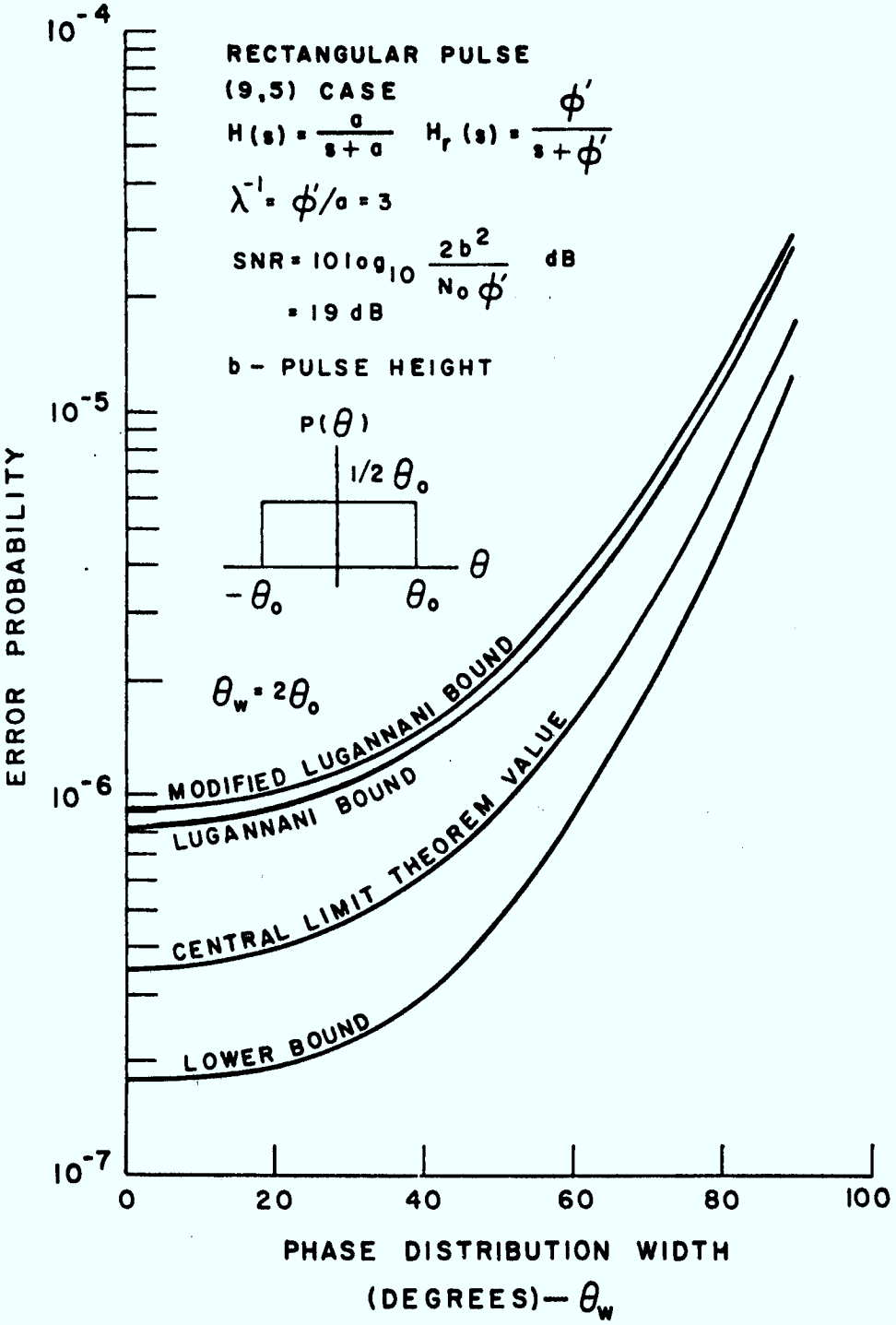


FIGURE 8: SYSTEM ERROR RATE DEGRADATION VERSUS UNIFORM PHASE DISTRIBUTION WIDTH - (9,5) CASE

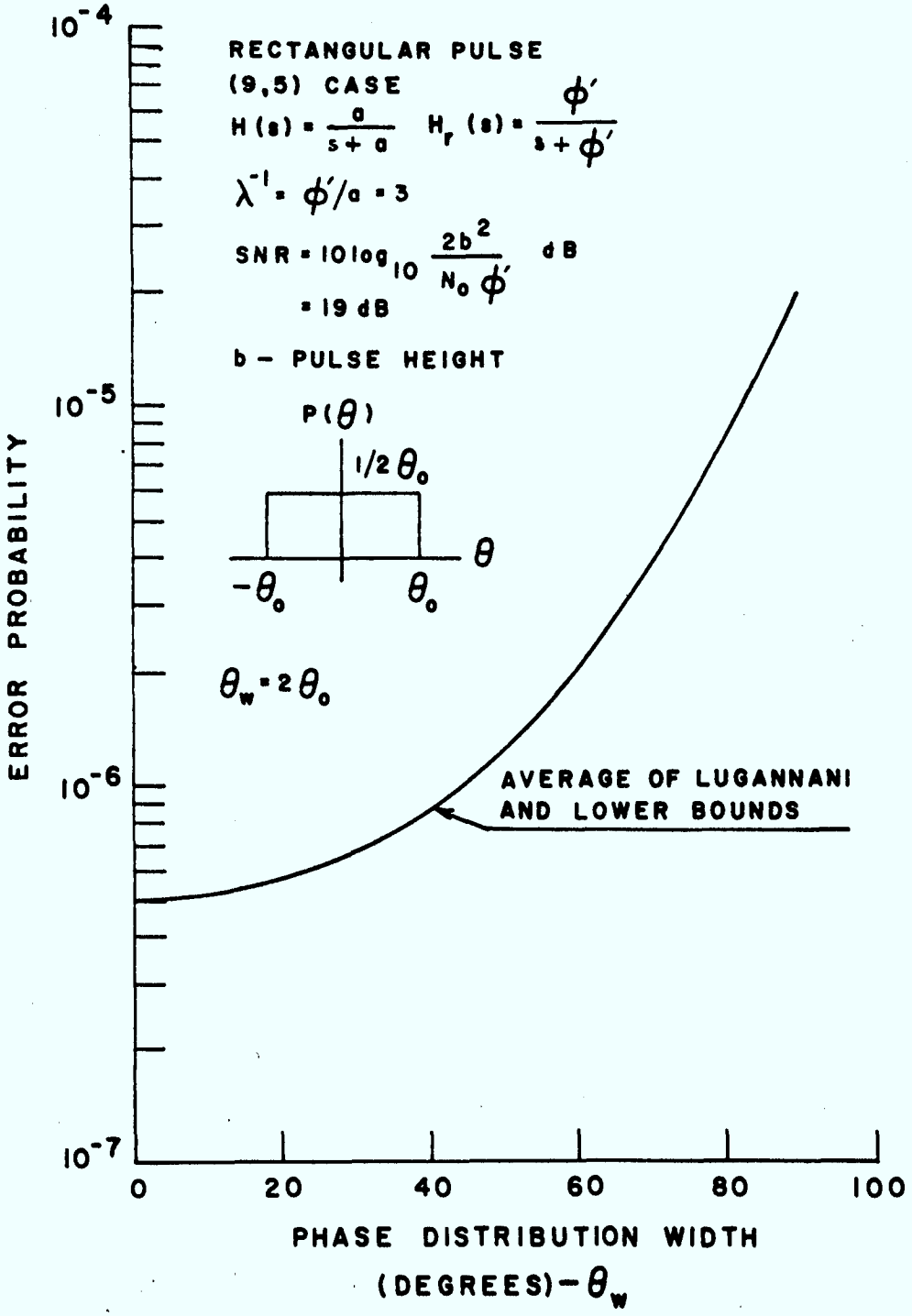


FIGURE 9: SYSTEM ERROR RATE DEGRADATION VERSUS UNIFORM PHASE DISTRIBUTION WIDTH - (9,5) CASE

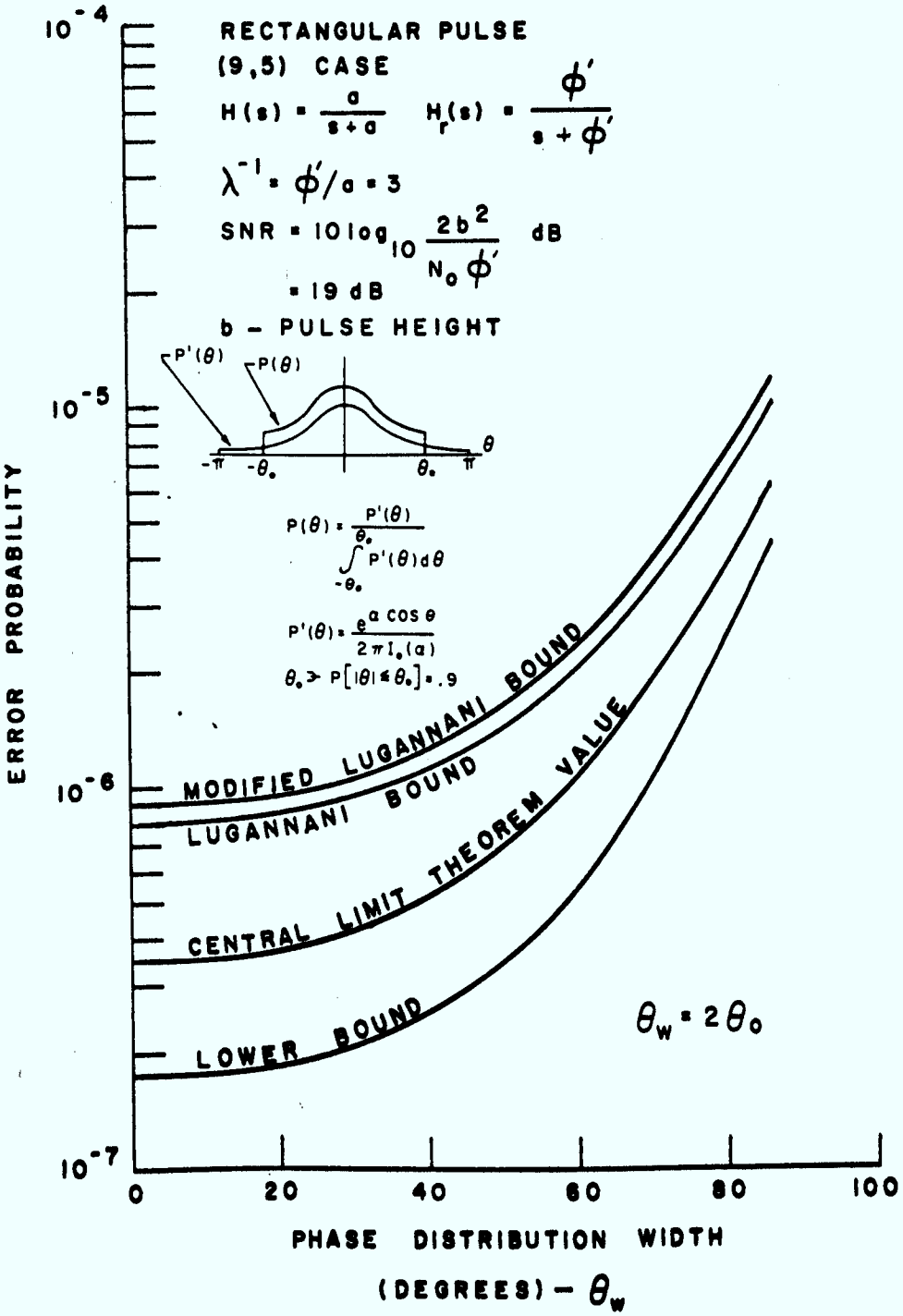


FIGURE 10: SYSTEM ERROR RATE DEGRADATION VERSUS NON-UNIFORM PHASE DISTRIBUTION WIDTH - (9,5) CASE

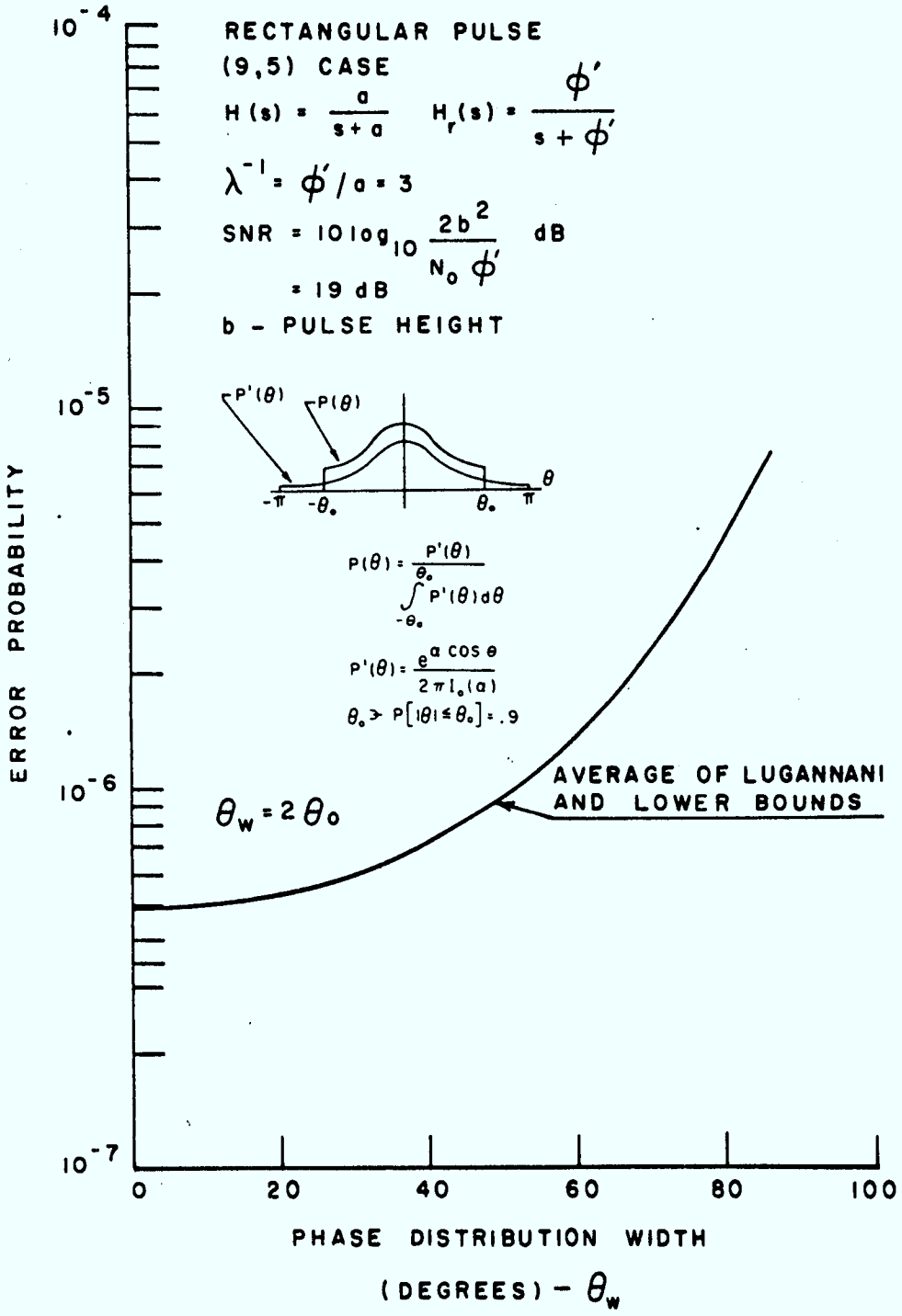


FIGURE 11: SYSTEM ERROR RATE DEGRADATION VERSUS NON-UNIFORM PHASE DISTRIBUTION WIDTH - (9,5) CASE

Assume that the incoherent receiver operates with $P_{AVG} = P_o$, where $P_o$ is the nominal error probability with SNR = $SNR_o$, when there is no phase uncertainty. If a phase is present in the carrier when SNR = $SNR_o$, then a new $P_{AVG}$ will be in effect. The difference in error probabilities, $\Delta P = |P_{AVG} - P_o|$, is to be made less than some tolerance $\varepsilon_T$. The proper choice of a new $\sigma^2$ will result in the determination of the necessary SNR by the inverse of the function which determines $\sigma^2$ in terms of the receiver structure and SNR. The difference, $\Delta SNR = SNR - SNR_o$, gives the additional SNR required to compensate for the phase uncertainty. The iterative search for the $\Delta SNR$ is depicted in Fig. 12.

Approximate Method

While the iterative method produces a $\Delta SNR$ determined by a specific tolerance on $\Delta P$, it may converge slowly depending on $\varepsilon_T$. An approximate technique may prove useful.

The lower bound is given by

$$P_{LB} = E_\theta \left\{ \text{erfc} \left[ \frac{\psi_{\alpha+1} \cos \theta}{\sigma} \right] \right\}$$

where $E_\theta[\cdot]$ denotes the expectation over $\theta$. An effective SNR is defined by

$$SNR_{eff} = \left[ \frac{\psi_{\alpha+1} \cos \theta}{\sigma} \right]^2$$

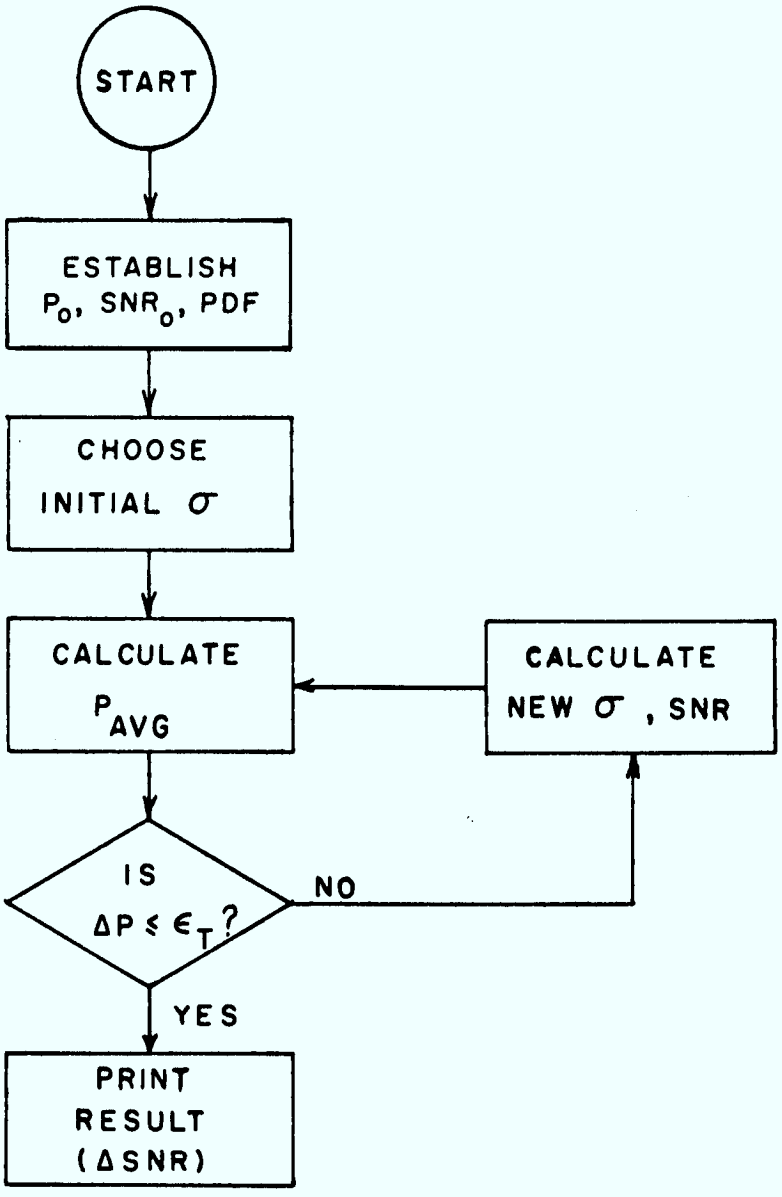


FIGURE 12: ITERATIVE SEARCH FOR PHASE COMPENSATING ΔSNR

whose expected value is given by

$$\overline{SNR}_{eff} = \frac{\psi^2_{\alpha+1}}{\sigma^2} \cdot E(\cos^2 \theta) \qquad (3.8.3)$$

Clearly, if $\sigma^2_{new} = E(\cos^2 \theta) \cdot \sigma^2$ for a given phase pdf then $\overline{SNR}_{eff}$ reduces to the nominal, zero-phase value. Hence, for a specified pdf, the determination of the needed SNR becomes trivial. Of course, this method is based on the argument of the lower bound and consequently an inherent error is present because $P_{AVG}$ is determined by both $P_L$ and $P_{LB}$. However, the ease of SNR calculation is appealing. The usefulness of this method can be verified by finding $\Delta P$ and comparing this value with $\varepsilon_T$.

## 3.9 SNR Adjustment Curves

Figure 13 gives the additional SNR required to compensate for varying uniform phase distribution widths for the (7,5) case. For the functional description of $\sigma^2$ see [4]. The numerical technique of Sec. 3.8 estimates that 4.5 dB are necessary when the phase width is 120°. Figure 14 compares the accuracy of the numerical and approximate methods. In this instance the approximate method is only useful for a maximum width of about 40°.

## 3.10 Example 2 Parameters

To assess the effect of a measured channel characteristic upon the system error rate performance, the parameters given by Falconer and Gitlin [13] will be used.

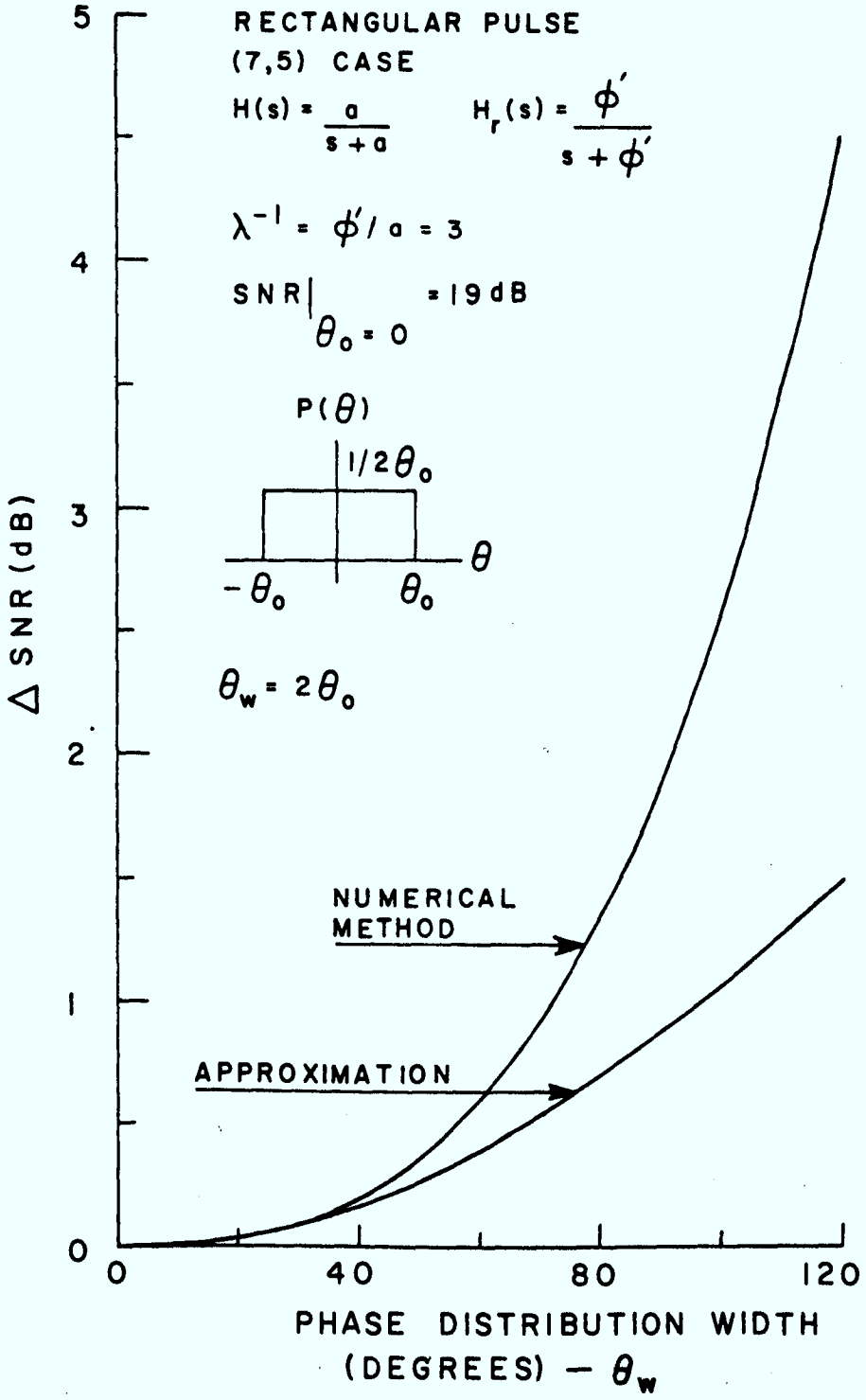


FIGURE 13: ADDITIONAL COMPENSATING SNR VERSUS UNIFORM PHASE DISTRIBUTION WIDTH

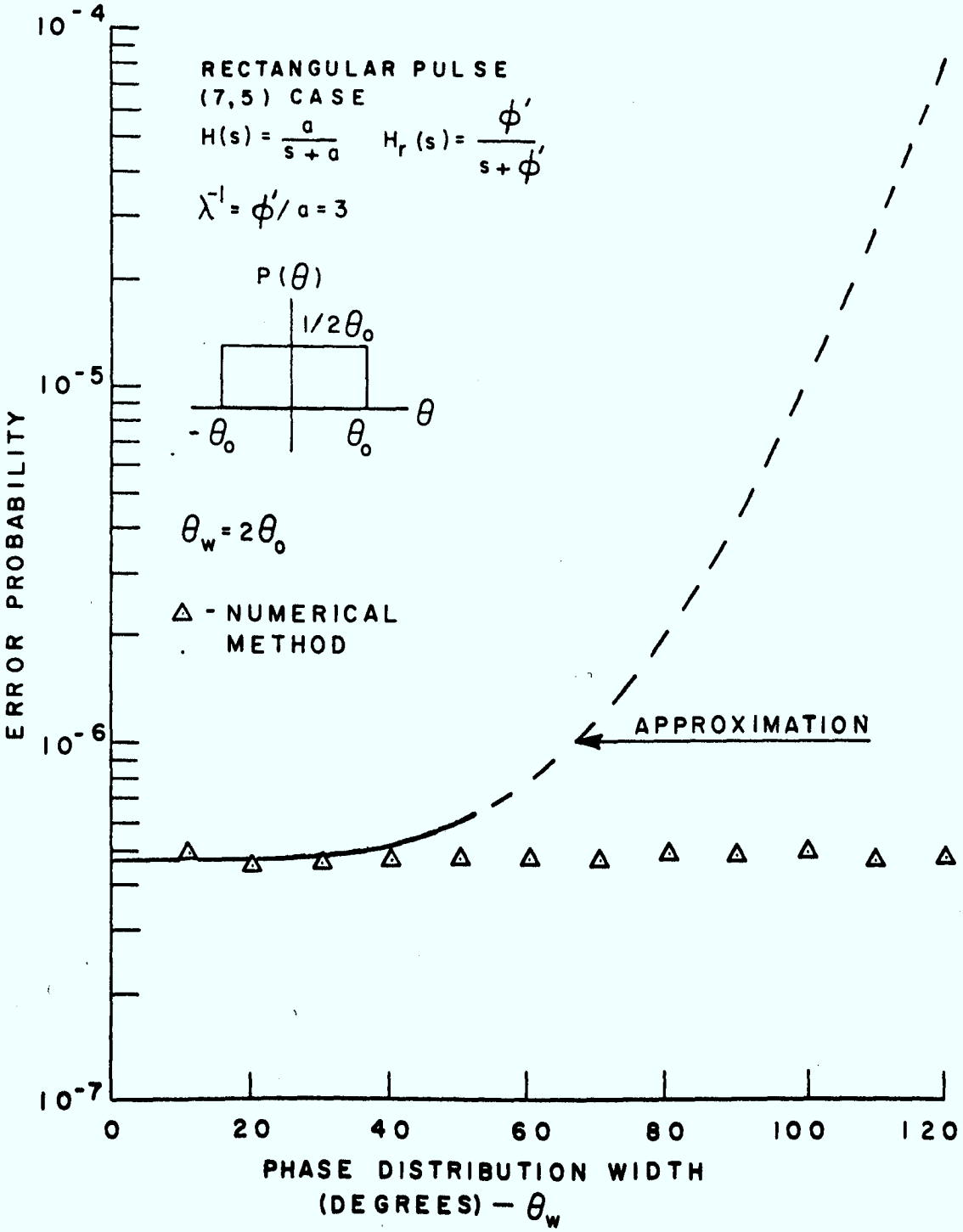


FIGURE 14: AVERAGE BOUND AFTER SNR ADJUSTMENT AS FUNCTION OF UNIFORM PHASE DISTRIBUTION WIDTH

First, a review of their receiver model will be given.

The $i^{th}$ sampled channel output is written as

$$y_i = \sum_j x_j \, \xi'_{i-j} + \eta_i$$

where the $\xi'_i$ are the input symbols absorbing cos $\theta$, the $x_i$ are the impulse response samples of the channel and the $\eta_i$ are statistically independent zero-mean Gaussian random variables with variance $\sigma^2$. The values taken by $j = \ldots, -1, 0, 1, 2, \ldots$ . The tap weights of a (2K+1)-tap transversal equalizer are given by

$$(C_{-K}, \ldots, C_o, \ldots, C_K)$$

The $i^{th}$ output sample of the equalizer is then

$$\hat{\xi}_i = \sum_{j=-K}^{K} C_j \, y_{i-j}$$

$$= \sum_\ell \xi'_\ell \, \psi_{i-\ell} + \gamma_i$$

$$= \sum_\ell \xi_\ell \, \psi'_{i-\ell} + \gamma_i$$

where

$$\psi'_i = \cos\theta \cdot \psi_i$$

and

$$\psi_i = \sum_{j=-K}^{K} C_j \, x_{i-j} \qquad i = \ldots, -1, 0, 1, 2, \ldots . \qquad (3.10.1)$$

is the overall channel-equalizer configuration impulse response. The term

$$\gamma_i = \sum_{j=-K}^{K} C_j \, \eta_{i-j}$$

represents the sequence of correlated Gaussian noise samples produced by the equalizer and the variance of $\gamma_i$ is given in [13] by

$$\sigma^2 = \sum_i x_i^2/SNR \qquad (3.10.2)$$

The information digit estimate is

$$\hat{\xi}_o = \sum_{j=-K}^{K} C_j \, y_{-j}$$

Using the minimum mean-square estimation error criterion (3.5.1) and the method of Lucky et al [2, p.141], it can be shown that the $C_i$ are given by solving

$$x_{-i} = \sum_{j=-K}^{K} C_j \, b_{i-j} \qquad (3.10.3)$$

with

$$b_i = \sum_{j=-\infty}^{\infty} \xi_j \, \xi_{j-i} + \sigma^2 \, \delta_{io}$$

and $\delta_{ik}$ is the Kronecker delta.

## 3.11 Performance and SNR Adjustment Curves - Example 2

The channel considered by Falconer and Gitlin [13, Example 1] - Channel 2 - can be represented by the impulse samples $x_i$ (truncated to 25 samples):

Impulse Response $\{x_i\}$ = {.002, -.001, 0., .001, -.008,
.01, -.028, .033, -.067, .126,
-.311, -.245, .806, .189, .265,
.051, .087, .014, .031, .009,
.011, .008, .004, .006, .002},

where $x_o$ = 0.806. With an SNR = 13 dB, the corresponding value of $\sigma$, by (3.10.2), is 0.215. Solving (3.10.3) for the $C_i$ and using these values in (3.10.1) gives the 39 values of $\psi_i$

$\underline{\psi}$ = {-.58E-04, .18E-03, -.15E-03, .29E-03, .15E-03,
-.29E-03, .19E-02, -.30E-02, .58E-02, -.16E-01,
.29E-01, -.45E-01, .51E-02, -.22E-01, .87E-02,
-.14E-01, .90E-02, -.10E-01, .80E-02, .95E 00,
.67E-02, -.66E-02, .54E-02, -.51E-02, .43E-02,
-.36E-02, .22E-02, -.27E-02, .48E-02, -.14E-02,
.24E-02, -.10E-02, -.21E-02, -.22E-03, -.11E-03,
-.90E-04, -.50E-04, -.36E-04, -.68E-05}

Figure 15 portrays the upper and lower bounds for this channel found by (3.6.1). The phase pdf is assumed uniform on the interval $[-\theta_o, \theta_o]$. The ordinate intercepts differ by less than an order-of-magnitude. The average of the Lugannani and lower bounds indicates that uniform phase distribution widths as large as $90^o$ are tolerable for this channel before the system error rate degrades by a factor of ten.

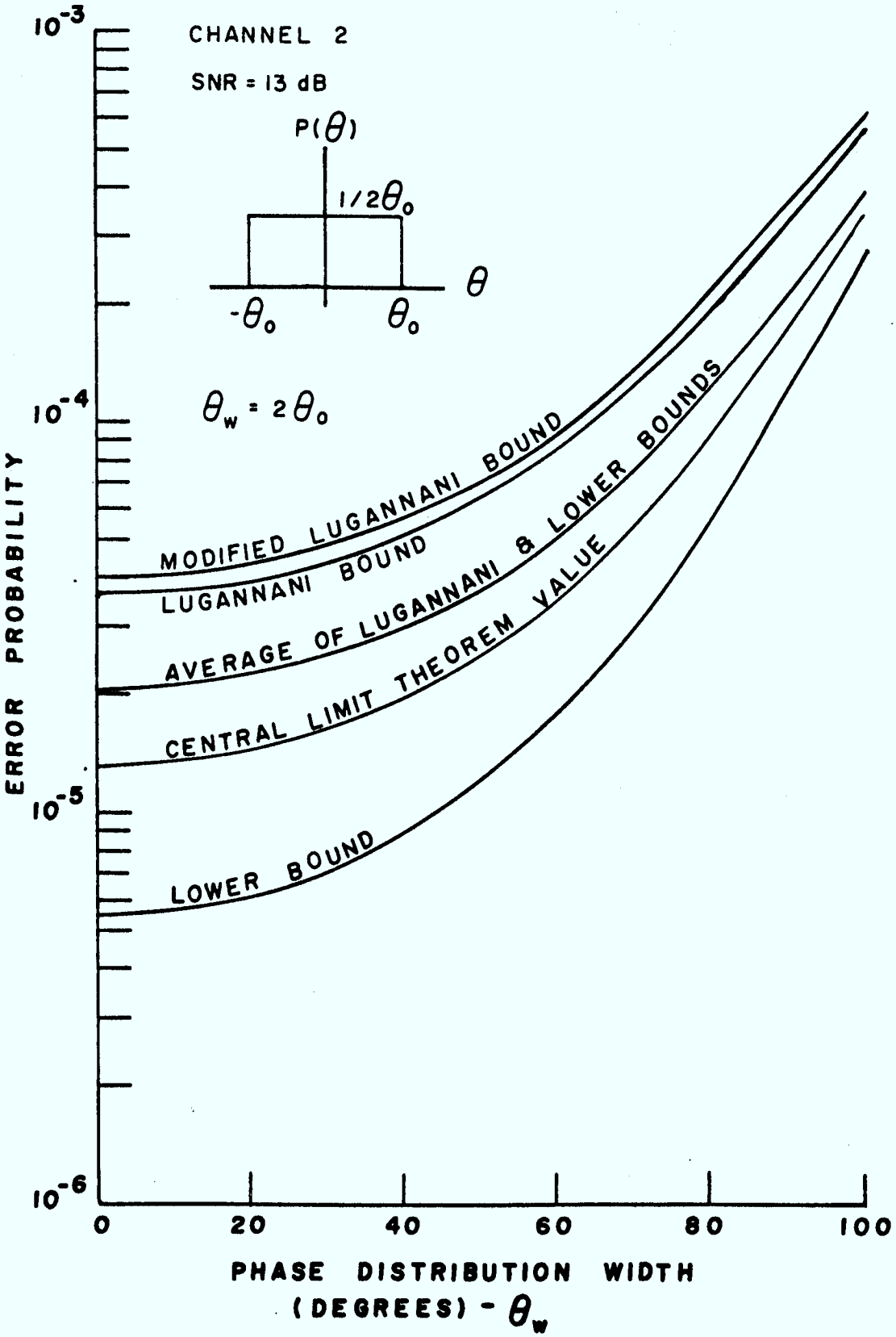


FIGURE 15: SYSTEM ERROR RATE DEGRADATION VERSUS UNIFORM PHASE DISTRIBUTION WIDTH - CHANNEL 2

Figure 16 depicts the additional SNR required to compensate for varying uniform phase distribution widths. Both the iterative and approximate methods described in Sec. 3.8 are applied to the Channel 2 situation. In the case of the iterative technique, the functional relation between the SNR and $\sigma$ is given by (3.10.2). The numerical technique estimates a 4 dB increase in SNR will compensate for a phase pdf width of 100°. Figure 17 compares the accuracy of the two methods and indicates that the approximate method is no longer useful for widths greater than about 50°.

## 3.12 Summary

This chapter has investigated the performance of a standard equalizer receiver when confronted by a phase uncertainty in the received signal carrier. Error bounds which were sufficiently close to localize the probability of digit error to within a neighbourhood of the true value were used for two types of phase pdf and phase distribution widths to 120°. Two channels were considered: a single-pole, time-dispersive channel and a measured sampled channel. A phase compensation technique involving increasing the SNR, without receiver modification, was investigated. The next two chapters are concerned with altering the receiver to permit tracking of the phase uncertainty.

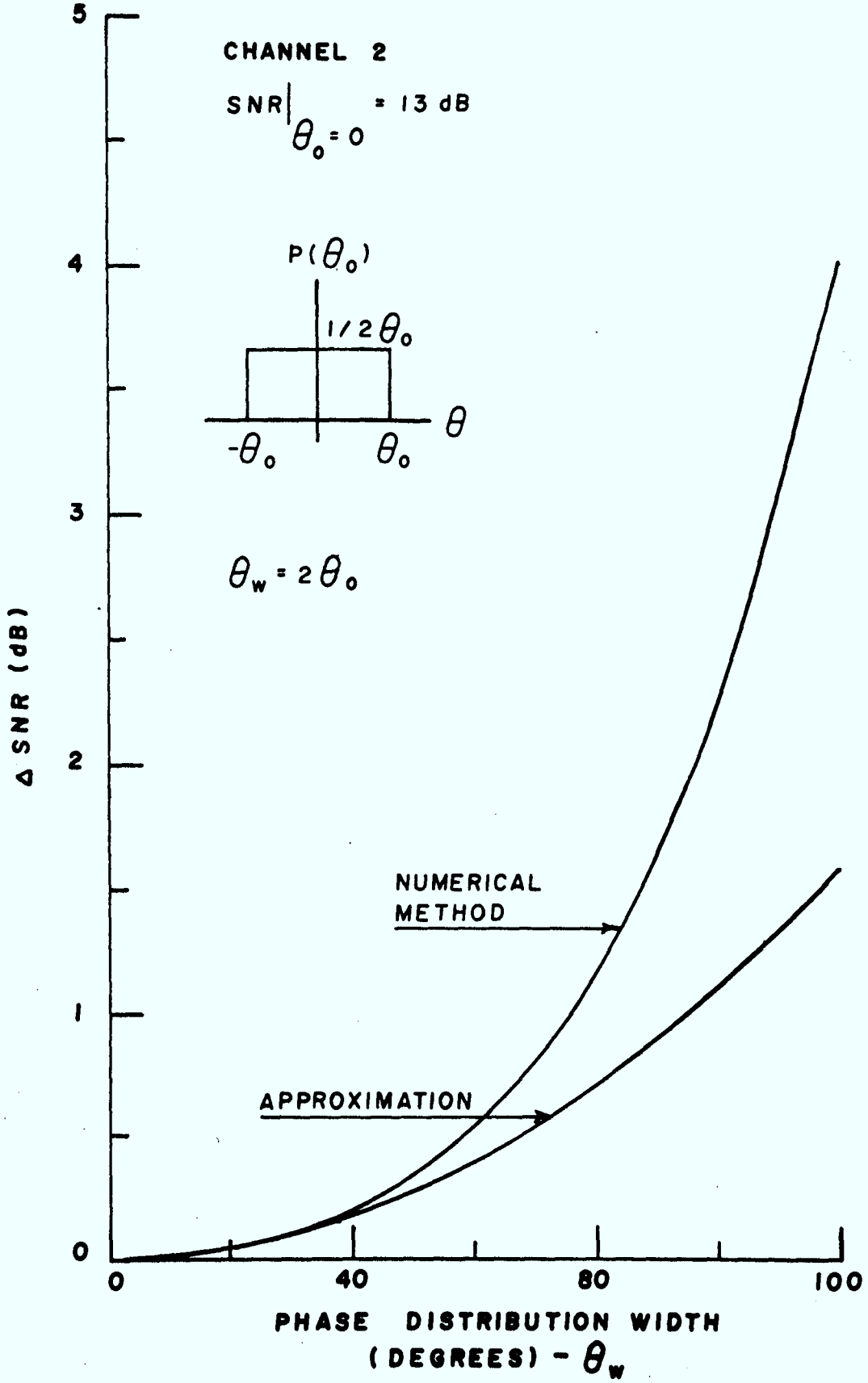


FIGURE 16: ADDITIONAL COMPENSATING SNR VERSUS UNIFORM PHASE DISTRIBUTION WIDTH - CHANNEL 2

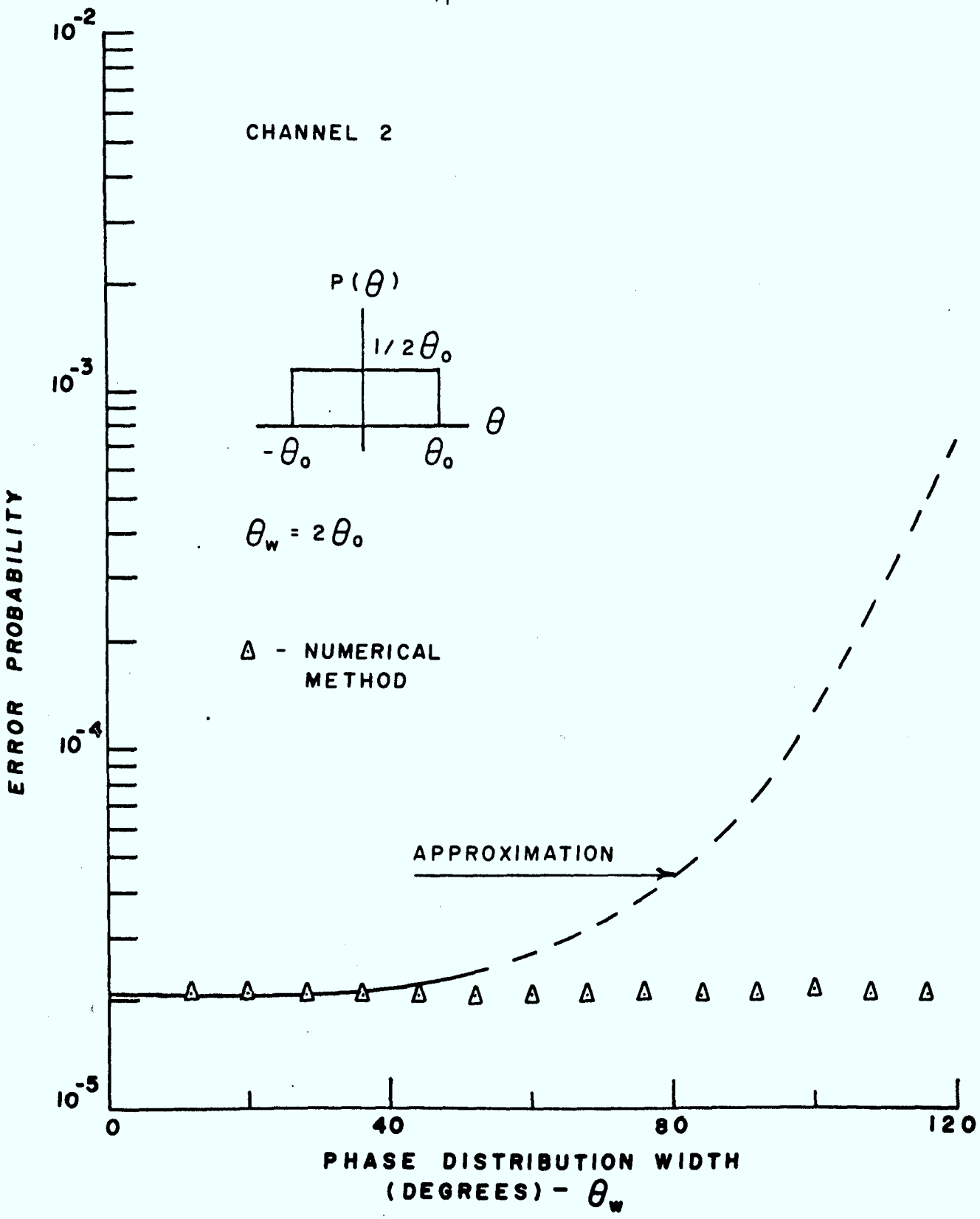


FIGURE 17: AVERAGE BOUND AFTER SNR ADJUSTMENT AS FUNCTION OF UNIFORM PHASE DISTRIBUTION WIDTH - CHANNEL 2

# CHAPTER 4

# THE COHERENT RECEIVER: THE PHASE-LOCKED LOOP

## 4.1 Introduction

The preceding chapter indicated that a degradation in system error rate performance occurs with increasing phase pdf width. While the P(error) may be tolerable for small distribution widths, larger values of the random phase $\theta$ result in unacceptable error rates. In an attempt to compensate for these larger phase values, tracking loops are included in the receiver. Tracking loops are designed so that the loop output is the difference between the loop phase estimate and the random phase $\theta$. The loop output has a pdf which assigns a large probability to small phase differences.

This chapter assesses receiver performance when a standard phase-locked loop (SPLL) is included with the baseband receiver of Sec. 3.2. After reconsidering the nature of the transmitted signal, the integro-differential equation governing loop operation will be derived. This will be followed by the pdf solution to the loop equation. Finally, the system error rate performance will be examined.

## 4.2 The Received Signal

To produce an estimate of $\theta$, the receiver requires information about the random phase. One method of generating this information is by transmitting a tone with the modulation [15, p. 262]. If the phase is due to a transmitter offset, then a tone harmonically related to the carrier and outside the modulation band can be used. If the phase is due to a channel disturbance, then tone bursts may be sent periodically from which a phase estimate applicable to the succeeding data stream interval may be produced. Although tracking loop operation is similar in both instances, the case of a phase arising from a transmitter offset will be treated here. This approach leads directly to the theory of Chap. 5. With this assumption the transmitted signal can be written as

$$x(t) = (2m^2P)^{\frac{1}{2}} \sin(\omega_c t+\theta) + [2(1-m^2)P]^{\frac{1}{2}} \cdot \sum_{n=0}^{N-1} \xi_n \, p(t-nT) \cos(\omega_m t+\theta)$$

where m is the modulation index indicating power allocation, P is root-mean-squared (rms) power and $\omega_c$ is the tone frequency. Assuming that the channel filter exhibits the same bandlimited response about both $\omega_c$ and $\omega_m$, the channel filter output may be considered as the linear combination of the following two terms:

$$y_1(t) = \sqrt{2} \int_0^t h^1(t-\tau)(m^2P)^{\frac{1}{2}} \sin(\omega_c\tau+\theta)d\tau \qquad (4.2.1)$$

$$y_2(t) = \sqrt{2} \int_0^t h^2(t-\tau)[(1-m^2)P]^{\frac{1}{2}} \cdot$$

$$\sum_{n=0}^{N-1} \xi_n \, p(\tau-nT) \cos\omega_m\tau d\tau \qquad (4.2.2)$$

where

$$h^1(t) = 2h_c(t)\cos\omega_c t$$

$$h^2(t) = 2h_c(t)\cos\omega_m t \ .$$

Writing (4.2.1) in complex form and using the identity

$$\text{Re } \alpha \cdot \text{Im } \beta = \frac{1}{2} \text{Im}[\alpha\beta - \alpha\beta^*] \ ,$$

$$y_1(t) = \sqrt{2} \, (m^2P)^{\frac{1}{2}} \int_0^t h_c(t-\tau) \cdot$$

$$\text{Im}\{e^{j(\omega_c t+\theta)} - e^{j(\omega_c t-\theta)} e^{-2j\omega_c\tau}\} \, d\tau$$

The double frequency term involving $\exp(-2j\omega_c\tau)$ may be neglected. Therefore,

$$y_1(t) = \sqrt{2} \, (m^2P)^{\frac{1}{2}} [\int_0^t h_c(t-\tau)d\tau] \sin(\omega_c t+\theta).$$

It will be further assumed that in the steady state

$$\int_0^t h_c(t-\tau)d\tau \to 1.$$

Hence,

$$y_1(t) = \sqrt{2} \, (m^2P)^{\frac{1}{2}} \sin(\omega_c t+\theta) \qquad (4.2.3)$$

Note that the form of (4.2.3) implies that the tone is undistorted by the channel filter.

Using the same procedure as in Sec. 2.3, (4.2.2) becomes

$$y_2(t) = \sqrt{2}\,[(1-m^2P]^{\frac{1}{2}} \sum_{n=0}^{N-1} \xi_n\, g(t-nT)\, \cos(\omega_m t+\theta) \qquad (4.2.4)$$

where

$$g(t) = h_c(t) \circ p(t) .$$

Adding Gaussian noise to the channel filter output gives for the received signal

$$y^1(t) = \sqrt{2}\,(m^2P)^{\frac{1}{2}} \sin(\omega_c t+\theta) + \sqrt{2}\,[(1-m^2)P]^{\frac{1}{2}} \cdot \sum_{n=0}^{N-1} \xi_n\, g(t-nT)\, \cos(\omega_m t+\theta) + n(t) \qquad (4.2.5)$$

where $n(t)$ is white over the band of interest and can be written as

$$n(t) = \sqrt{2}\,[n_1(t)\, \cos\omega_c t - n_2(t)\, \sin\omega_c t] \qquad (4.2.6)$$

## 4.3 Loop Operation

The SPLL tracking device is depicted in Fig. 18. The received signal $y^1(t)$ is multiplied by the VCO reference signal $r(t)$ where

$$r(t) = \sqrt{2}\, \cos\, \hat{\Phi}(t)$$

where $\hat{\Phi}(t) = \omega_c t+\hat{\theta}$ and $\hat{\theta}$ is the loop phase estimate. A

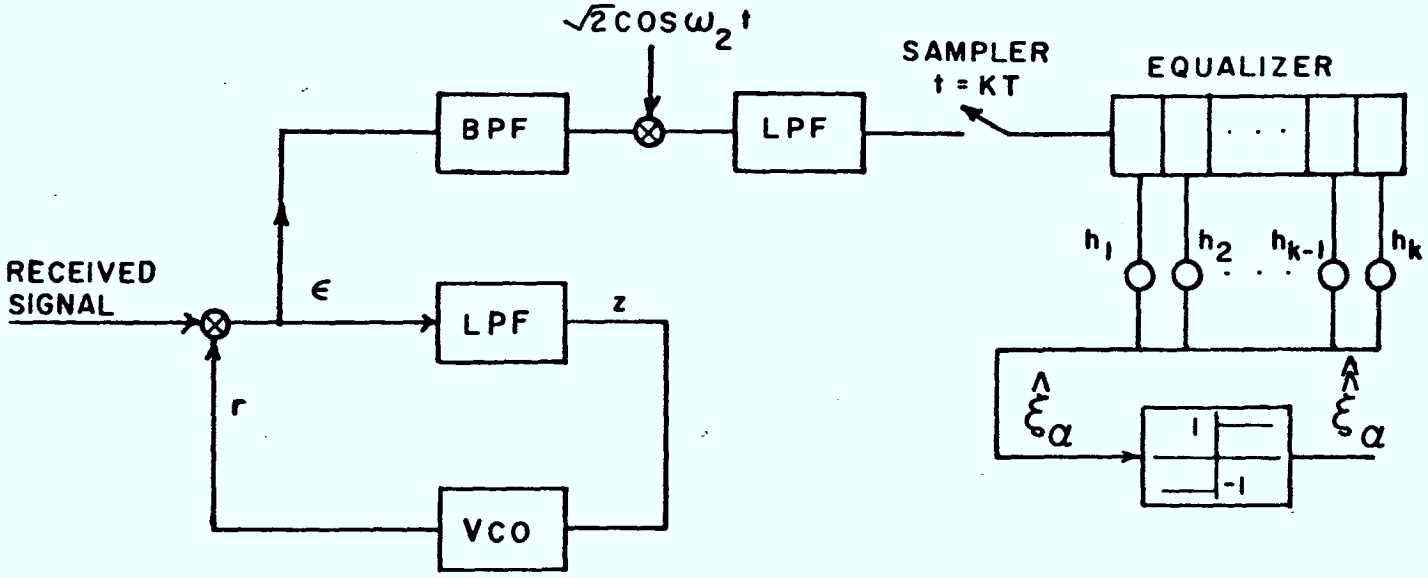


FIGURE 18: COHERENT RECEIVER : SPLL WITH PAM RECEIVER

tap is taken after the multiplier and the multiplier output is demodulated to baseband before being processed by the equalizer circuit. In the loop the signal $\varepsilon(t)$ is passed through a low-pass filter (LPF) which removes out-of-band terms. The error-control signal $z(t)$ is then the input to the voltage-controlled oscillator (VCO).

Multiplying $y^1(t)$ by $r(t)$ gives for the loop multiplier output

$$\varepsilon(t) = r(t)\, y^1(t)$$

$$= \sqrt{2} \cos \Phi \{\sqrt{2}\, (m^2P)^{\frac{1}{2}} \sin(\omega_c t+\theta) + \sqrt{2}\, [(1-m^2)P]^{\frac{1}{2}} \cdot$$

$$\sum_{n=0}^{N-1} \xi_n\, g(t-nT) \cos(\omega_m t+\theta) + n(t)\} \qquad (4.3.1)$$

Expanding (4.3.1) as in Sec. 3.2 and neglecting double-frequency terms gives

$$\varepsilon(t) = (m^2P)^{\frac{1}{2}} \sin \phi + [(1-m^2)P]^{\frac{1}{2}} \sum_{n=0}^{N-1} \xi_n\, g(t-nT) \cdot$$

$$\{\cos [(\omega_c+\omega_m)t + \hat{\theta} + \theta] + \cos [(\omega_m-\omega_c)t + \phi]\}$$

$$+ n_1(t) \cos \hat{\theta} + n_2(t) \sin \hat{\theta} \qquad (4.3.2)$$

where $\phi = \theta - \hat{\theta}$ and the argument t of $\phi$ is suppressed. Viterbi [16] has shown that

$$n^1(t) = n_1(t) \cos \hat{\theta} + n_2(t) \sin \hat{\theta}$$

is essentially white and is characterized by the same statistics as $n_1(t)$ and $n_2(t)$. The LPF removes from $\varepsilon(t)$ the terms at $\omega_m \pm \omega_c$ and hence $z(t)$ may be written in operator form [9,11] as

$$z(t) = F(s) \{(m^2P)^{\frac{1}{2}} \sin \phi + n^1(t)\}$$

where $F(s)$ is the LPF filter function.

The VCO output phase $\hat{\theta}$ is related to its input by

$$\hat{\theta} = \frac{K}{s} z$$

$$= \frac{K}{s} \{F(s) [(m^2P)^{\frac{1}{2}} \sin \phi + n^1(t)]\} \qquad (4.3.3)$$

Noting that $\phi = \theta - \hat{\theta}$ and differentiating (4.3.3) yields

$$\dot{\phi} = \dot{\theta} - K F(s) [(m^2P)^{\frac{1}{2}} \sin \phi + n^1(t)].$$

Here, $\dot{\theta} = 0$, the no-detuning situation, and therefore

$$\dot{\phi} = - K F(s) [(m^2P)^{\frac{1}{2}} \sin \phi + n^1(t)] \qquad (4.3.4)$$

which represents the stochastic integro-differential equation governing loop operation.

## 4.4 Nonlinear Analysis of the First-Order SPLL

When $F(s)$ is first-order, i.e., $F(s)$ has unit gain, (4.3.4) becomes

$$\dot{\phi} = - K[(m^2P)^{\frac{1}{2}} \sin \phi + n^1(t)] \qquad (4.4.1)$$

The pdf of $\phi$ may be obtained by invoking the Fokker-Planck equation [7, p.86]. For the stochastic differential equation

$$\dot{\phi} = P(\phi) + \sqrt{G(\phi)}\ \underline{n}(t) \tag{4.4.2}$$

where $\underline{n}(t)$ is Gaussian white noise, the Fokker-Planck equation is

$$\frac{\partial p(\phi,t)}{\partial t} = -\frac{\partial}{\partial \phi} P(\phi)\ p(\phi) + \frac{N_o}{4} \frac{\partial^2 G(\phi) p(\phi)}{\partial \phi^2} \tag{4.4.3}$$

where $N_o/2$ is the two-sided spectral height of $\underline{n}(t)$. Here, the steady state (i.e., $\frac{\partial p}{\partial t} = 0$), modulo $2\pi$ solution is of interest. Therefore, (4.4.3) becomes

$$\frac{d}{d\phi} G(\phi)\ p(\phi) - \frac{4}{N_o} P(\phi)\ p(\phi) = C \tag{4.4.4}$$

Comparing (4.4.1) and (4.4.2) yields

$$P(\phi) = -K(m^2 P)^{\frac{1}{2}} \sin \phi$$

$$G(\phi) = K^2$$

Using these results in (4.4.4), integrating and invoking the boundary condition $p(\pi) = p(-\pi)$ yields [7, p. 92]

$$p(\phi) = \frac{\exp(\alpha \cos\phi)}{2\pi I_o(\alpha)} \tag{4.4.5}$$

where

$$\alpha = \frac{A'^2}{N_o(A'K/4)}\ ,\ A' = (m^2 P)^{\frac{1}{2}} \tag{4.4.6}$$

and $\alpha$ is the loop SNR. The term $B = A'K/4$ is the loop bandwidth of the first-order loop. The denominator term $I_o(\alpha)$ is the modified Bessel function of zero-order and argument $\alpha$. Note that if $\alpha = 0$, the phase pdf is uniform. Reference [7, p.91] depicts $p(\phi)$ versus several values of the parameter $\alpha$.

## 4.5 SPLL Performance Curves

A tap is taken after the loop multiplier. This tap represents the desired phase-compensated modulation. The modulation is passed through a bandpass filter BPF which extracts the term

$$y''(t) = [(1-m^2)P]^{\frac{1}{2}} \sum_{n=0}^{N-1} \xi_n \, g(t-nT) \cos[(\omega_m-\omega_c)t + \phi] + n'_{BP}(t) \qquad (4.5.1)$$

where $n'_{BP}(t)$ is filtered white noise with spectral height $N_o/2$ watts/Hz. To present the equalizer with a low-pass signal $y''(t)$ must be demodulated to baseband. Hence, the BPF output is multiplied by $\sqrt{2} \cos \omega_2 t$ where $\omega_2 = \omega_m - \omega_c$. The demodulator output, neglecting high frequency terms which will not be passed by the equalizer LPF, is then

$$y'(t) = [(1-m^2)P']^{\frac{1}{2}} \sum_{n=0}^{N-1} \xi_n \, g(t-nT) \cos\phi + n''(t) \qquad (4.5.2)$$

where $P = 2P'$ and $n''(t)$ is Gaussian noise with spectral height $N_o/2$ watts/Hz.

The form of (4.5.2) is the same as that signal presented to the incoherent receiver of Sec. 3.2 except that the random phase $\theta$ has been replaced by the error phase $\phi$ as the cosine argument. When the statistics of $\phi$ have been determined by proper loop design, i.e., $\phi$ is non-uniform, then receiver performance can be expected to improve.

In this case the detected equalizer $SNR_E$ will be

$$SNR_E \triangleq 10 \log_{10} \frac{b^2}{N_o \phi'} \text{ dB}$$

$$= 10 \log_{10} \left[\frac{(1-m^2)P'}{N_o \phi'}\right] \text{ dB} \qquad (4.5.3)$$

where $\phi'$ is the one-sided equalizer bandwidth. The SPLL SNR is given by

$$\rho = 10 \log_{10} \left[\frac{m^2 P}{N_o B}\right] \qquad (4.5.4)$$

For a fixed equalizer $SNR_E = C$, a modified form of (4.5.4) can be obtained. Solving for $P = 2P'$ in (4.5.3) yields

$$P = \frac{2}{(1-m^2)} N_o \phi' 10^{C/10} \qquad (4.5.5)$$

Substituting for P in (4.5.4) gives

$$\rho = 10 \log_{10} \left[\frac{2(m^2)}{(1-m^2)} \frac{\phi'}{B} \cdot 10^{C/10}\right] \qquad (4.5.6)$$

$$= 10 \log_{10} 2 + 10 \log_{10} \left(\frac{m^2}{1-m^2}\right) + 10 \log_{10} \frac{\phi'}{B} + C$$

$$= 10 \log_{10} \alpha \ .$$

Hence, the loop SNR becomes a function of three parameters: the modulation index, the equalizer-to-loop bandwidth ratio and the equalizer SNR.

The system error rate is assessed in the same manner as in Chap. 3 except that the phase pdf is now given by (4.4.5). Figures 19 and 20 portray the variation of the error probability as a function of the modulation index for three values of the parameter $\phi'/B$ for the two channels discussed in Chap. 3. Both Figures 19 and 20 indicate that the larger $\phi'/B$ the better will be the error rate performance. In addition, increasing the modulation index and consequently the tone power will reduce the average error probability.

The receiver exhibits the same performance when the transmitted signal consists of a synchronization waveform followed by the modulation:

$$s(t) = \begin{cases} \text{synchronization signal} & 0 \leq t \leq T_S \\ \text{modulation} & T_S \leq t \leq T_{NSI} \end{cases}$$

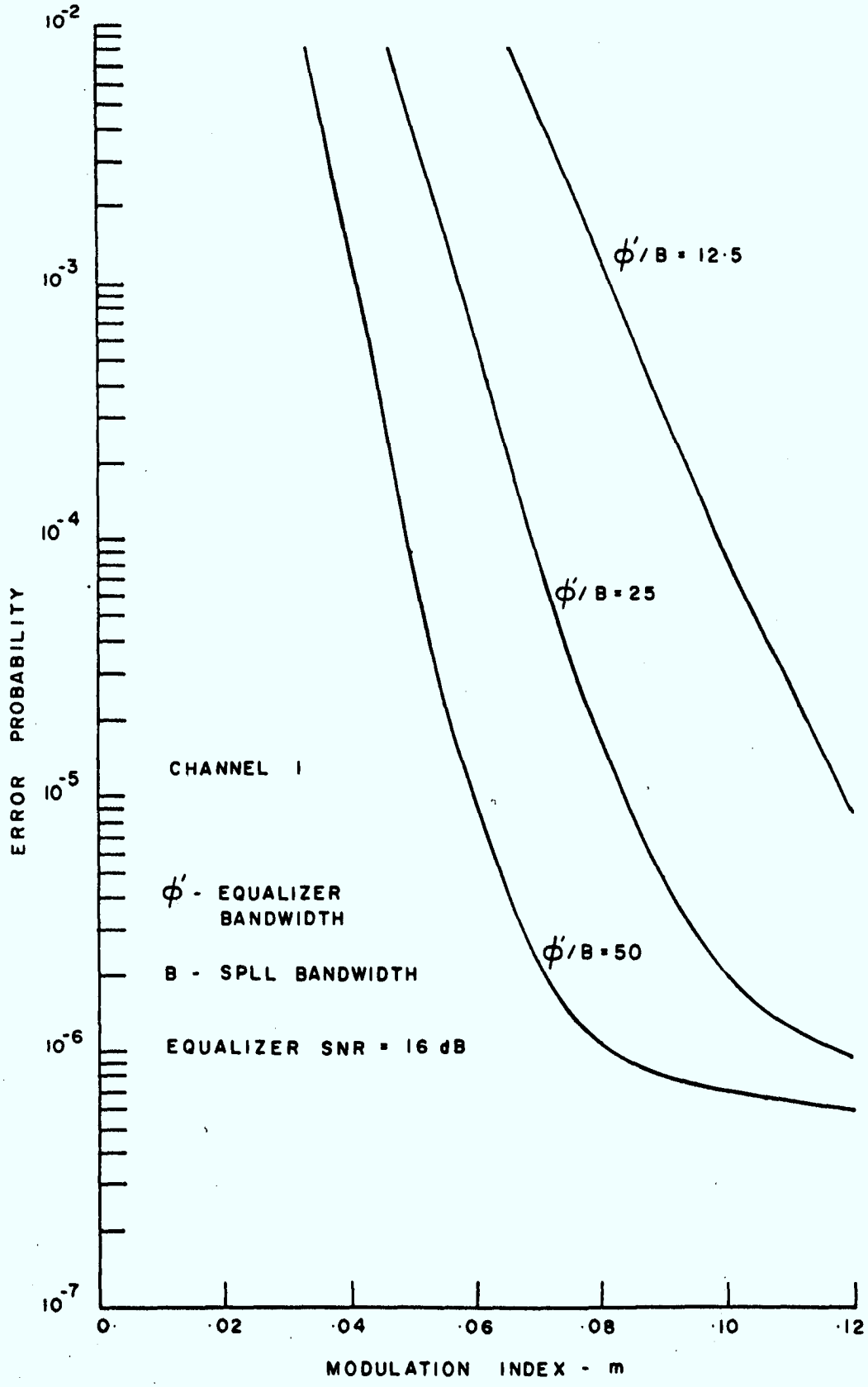


FIGURE 19: COHERENT RECEIVER ERROR RATE DEGRADATION - CHANNEL 1

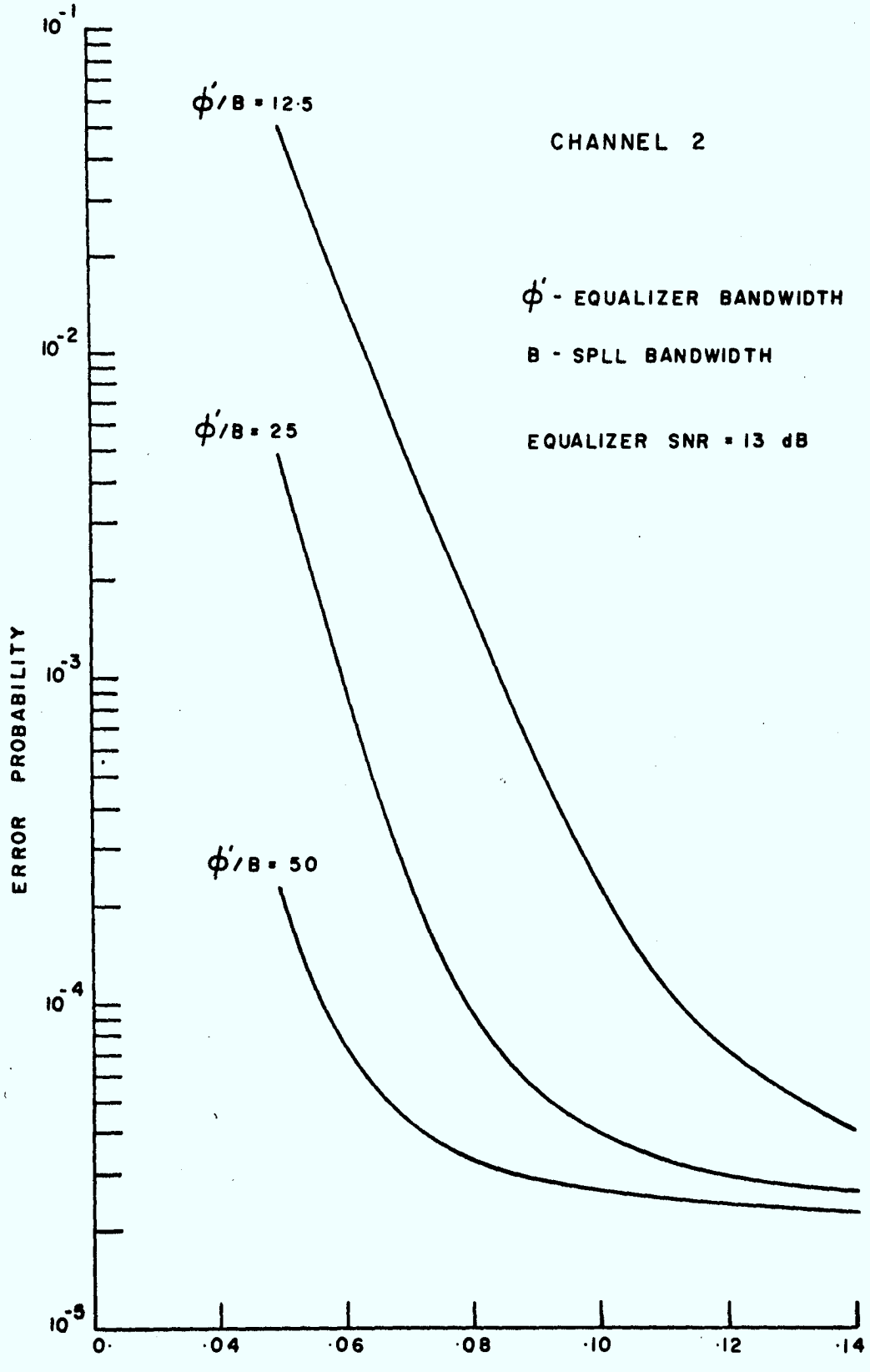


FIGURE 20: COHERENT RECEIVER ERROR RATE DEGRADATION - CHANNEL 2

where $T_S$ denotes the end of the synchronization and $T_{NSI}$ represents the start of the next synchronization interval. Here there is no power allocation between carrier and modulation and hence, m = 0. The synchronization signal, which may be a tone, is used by the SPLL to produce an estimate of the random phase for the modulation ON period. As the modulation has negligible content in the loop bandwidth it will not significantly alter the SPLL output.

## 4.6 Summary

The operation of a coherent receiver consisting of a series connection of a phase-locked loop and the standard equalizer for baseband PAM transmission has been examined for two sample channels. It has been shown that with a random input phase uniform on $[-\pi, \pi]$ that proper selection of the SPLL signal-to-noise ratio will effectively compensate for the phase distortion.

# CHAPTER 5

# THE COHERENT RECEIVER: THE DATA-AIDED CARRIER TRACKING LOOP

## 5.1 Introduction

The operation of the SPLL discussed in the preceding chapter was based not on the modulated signal but on a reference carrier. In their recent paper, Lindsey and Simon [11] introduced a data-aided demodulator which utilizes both modulation and carrier power to establish a coherent loop reference signal. Using the principle of decision-directed feedback, the data demodulator estimate is returned to the carrier tracking loop to enable recovery of the sideband component power for tracking purposes. The channel considered in [11] is applicable to digital transmission problems when the system data rate is less than that associated with the usable channel bandwidth.

The principal theoretical result of this chapter is the solution of the Fokker-Planck equation for the probability density function of the tracking loop phase error. The phase pdf solution is based on the assumption that the modulation is distorted by intersymbol interference,

phase jitter and additive Gaussian noise. Including the effect of intersymbol interference on the loop pdf solution represents an extension of the study by [11].

This examination is subject to the condition that the data-aided carrier tracking loop is of the first-order type. This implies that the only baseband filtering introduced in the tracking loop is achieved by the loop voltage-controlled oscillator (VCO). An estimate of the overall system error rate is obtained by averaging the conditional upper and lower bounds over the loop pdf. The bounds used were found to agree to within one order of magnitude.

## 5.2 Loop Operation

The received signal is as in (4.2.5):

$$y^1(t) = \sqrt{2}\,(m^2P)^{\frac{1}{2}} \sin(\omega_c t+\theta) + \sqrt{2}\,[(1-m^2)P]^{\frac{1}{2}} \sum_{n=0}^{N-1} \xi_n\, g(t-nT) \cdot \cos(\omega_m t+\theta) + n(t) \qquad (5.2.1)$$

where $\omega_c$ and $\omega_m$ are harmonically related for ease of implementation. The modulation centre frequency and reference carrier must be at different frequencies in order to obtain the decoupling that is required in the tracking loop. The carrier phase, $\theta$, is a slowly varying random process and is taken to be uniform on $[-\pi, \pi]$.

The channel receiver is illustrated in Fig. 21. The upper loop variables are those subscripted with "u"

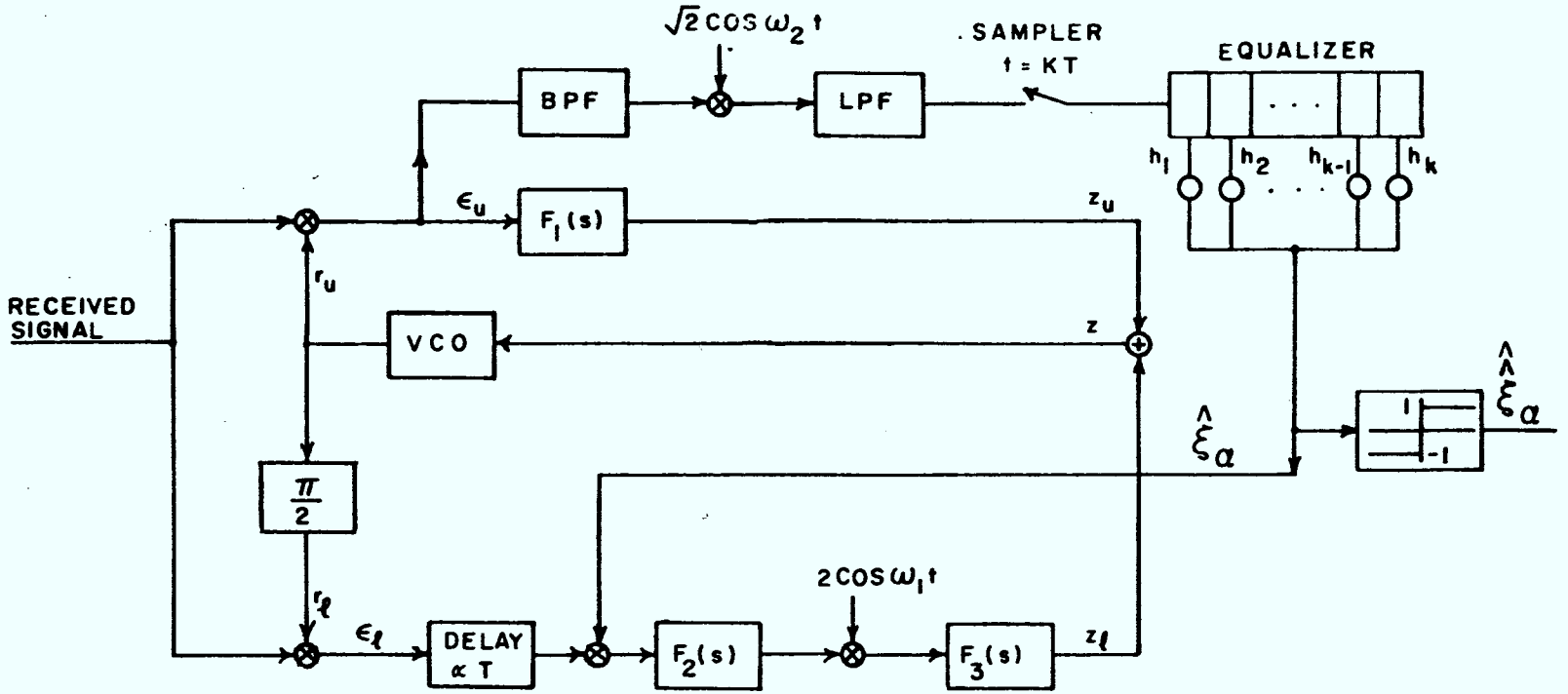


FIGURE 21: COHERENT RECEIVER : DATA-AIDED CARRIER TRACKING LOOP WITH PAM RECEIVER

and the lower loop variables are those subscripted with "ℓ". The tracking loop demodulates the received signal to baseband using two quadrature reference signals. One channel contains only tracking information, while the other channel contains both data and tracking signals. The data demodulator estimate $\hat{\xi}_\alpha$ is coupled into the lower loop in order to supply a non-zero power to the VCO from the lower loop. In the absence of this feedback the lower loop output is small. This is due to the fact that the modulation bandwidth greatly exceeds that of the carrier phase variations and as this latter bandwidth determines the lower loop bandwidth, the filters would average the modulation to a negligible value.

The upper loop analysis is almost identical to the SPLL analysis of Sec. 4.3. Here, the upper loop reference signal is

$$r_u(t) = \sqrt{2}\, K_1 \cos \hat{\Phi}$$

where $\hat{\Phi} = \omega_c t + \hat{\theta}$ and $\hat{\theta}$ is the loop phase estimate. Assuming an upper loop multiplier gain of $K_{1m}$, $\varepsilon_u(t)$ becomes

$$\begin{aligned}\varepsilon_u(t) &= \sqrt{2}\, K_1 K_{1m} \cos \hat{\Phi}\, y^1(t) \\ &= \sqrt{2}\, K_1 K_{1m} \cos \hat{\Phi} \{\sqrt{2}\, (m^2 P)^{\frac{1}{2}} \sin(\omega_c t+\theta) \\ &\quad + \sqrt{2}\, [(1-m^2)P]^{\frac{1}{2}} \sum_{n=0}^{N-1} \xi_n\, g(t-nT) \cdot \\ &\quad \cos(\omega_m t+\theta) + n(t)\}\end{aligned} \tag{5.2.2}$$

The random process n(t) is as before:

$$n(t) = \sqrt{2}\,[n_1(t)\cos\omega_c t - n_2(t)\sin\omega_c t]$$

$F_1(s)$ is a low-pass filter and hence double frequency terms and terms about $\omega_c \pm \omega_m$ in (5.2.2) may be neglected. Substituting for n(t) in (5.2.2) and expanding the trigonometric products gives

$$\varepsilon_u(t) = K_1 K_{1m}\,[(m^2P)^{\frac{1}{2}}\sin\phi + n'(t)]$$

where $\phi = \theta - \hat{\theta}$ is the loop phase error and n'(t) is white Gaussian noise. Hence, the upper loop filter output is

$$z_u(t) = K_1 K_{1m} F_1(s)\,[(m^2P)^{\frac{1}{2}}\sin\phi + n'(t)] \qquad (5.2.3)$$

A tap is taken after the upper loop multiplier. A bandpass filter extracts the tap output centred about $\omega_c-\omega_m$ and the filter output is demodulated to baseband using $\frac{\sqrt{2}}{K_1K_{1m}}\cos\omega_2 t$† where $\omega_2 = \omega_c-\omega_m$. The signal presented to the equalizer is then

$$y(t) = [(1-m^2)P']^{\frac{1}{2}} \sum_{n=0}^{N-1} \xi_n\, g(t-nT)\cos\phi + n'(t)$$

where $P' = P/2$.

The lower loop reference signal is

$$r_\ell(t) = -\sqrt{2}\,K_2\sin\hat{\Phi} \qquad (5.2.4)$$

The first stage of the lower loop filtering is taken to be centred around $\omega_c-\omega_m$ and is assumed to suppress carrier

†It is assumed that any error in oscillator phase does not significantly affect performance.

and d.c. terms outside a bandwidth around this centre frequency. Thus, using (5.2.1) and (5.2.4), the lower loop multiplier output is

$$\varepsilon_2(t) = - K_2 K_{2m} [(1-m^2)P]^{\frac{1}{2}} \sum_{n=0}^{N-1} \xi_n g(t-nT) \cdot$$

$$\sin [(\omega_c-\omega_m)t-\phi] - \sqrt{2} K_2 K_{2m} \sin \hat{\Phi} n(t) \quad (5.2.5)$$

where $K_{2m}$ is the lower loop multiplier gain. Equation (5.2.5) indicates that the tracking information is drawn from the modulation. The signal $\varepsilon_2(t)$ is delayed by an amount equal to the data demodulator delay so that the detected information bit $\hat{\xi}_\alpha$ can multiply (5.2.5). [The statistics of the unquantized estimate $\hat{\xi}_\alpha$ are easily obtained from (3.2.11). Using $\hat{\hat{\xi}}_\alpha$ for feedback purposes would complicate the derivation of the loop equation as the nonlinear operation of quantization makes finding the statistics of $\hat{\hat{\xi}}_\alpha$ difficult.] If the demodulator is working well, the multiplication effectively removes the modulation in (5.2.5) for the information bit, $\xi_\alpha$, but not the intersymbol interference, $\xi_i$, $i \neq \alpha$.

While the delay is necessary to ensure multiplication of $\xi_\alpha$ by its estimate $\hat{\xi}_\alpha$, it will be assumed that the delay has negligible effect upon the steady-state output of the filter $F_2(s)$ [11]. Thus, the output of the filter $F_2(s)$ is

$$f_\ell(t) = K_2\ K_{2m}\ F_2(s)\ \{[(1-m^2)P]^{\frac{1}{2}} \sum_{n=0}^{N-1} \xi_n\ \hat{\xi}_\alpha\ g(t-nT) \cdot$$

$$\sin\ [(\omega_m-\omega_c)t+\phi] - \sqrt{2}\ \hat{\xi}_\alpha\ \sin\ \hat{\Phi}\ n(t)\} \qquad (5.2.6)$$

When the loop bandwidth is small with respect to the bit rate the loop filter $F_3(s)$ effectively averages [11] the modulation terms in (5.2.6). In Sec. 3.2 it was shown that the data demodulator output is given by

$$\hat{\xi}_\alpha = \cos\ \phi\ \psi_{\alpha+1}\ \xi_\alpha + \cos\ \phi \sum_{\substack{i=0 \\ i\neq\alpha}}^{N-1} \xi_i\ \psi_{i+1} + \gamma \qquad (5.2.7)$$

where $\theta$ has been replaced by $\phi$ in (3.2.11), the $\psi_i$'s are constant and $\gamma$ is a Gaussian random variable. Thus,

$$E\{\hat{\xi}_\alpha\ \xi_i\} = \psi_{i+1}\ \cos\ \phi \qquad (i \leq \alpha)$$

and the fact that $i \leq \alpha$ indicates that the lower loop is not affected by any of the non-demodulated digits. Hence, demodulating $f_\ell(t)$ to baseband using $2\ \cos\ \omega_1 t$ where $\omega_1 = \omega_m-\omega_c$ and recalling the averaging introduced by $F_3(s)$, gives for $z_\ell(t)$

$$z_\ell(t) = \tfrac{1}{2}\ K_2\ K_{2m}\ F_3(s)\ \{[(1-m^2)P]^{\frac{1}{2}}\ A\ \sin\ 2\ \phi + n''(t)\} \qquad (5.2.8a)$$

where

$$A = \sum_{i=1}^{\alpha+1} \psi_i\ C_i \qquad (5.2.8b)$$

with

$$C_i = \frac{1}{T} \int_0^T g[t + (\alpha+1-i)]dt \qquad (5.2.8c)$$

and n"(t) is Gaussian white noise with spectral height

$$N_\phi = N_o[\underline{\sigma}_d^2 \cos^2 \phi + \sigma^2], \quad \underline{\sigma}_d^2 = \sum_{i=0}^{N-1} \psi_{i+1}^2 \qquad (5.2.8d)$$

while $\sigma^2$ is the variance of $\gamma$, the zero mean Gaussian random variable in (5.2.7). The form of n"(t) arises as the last term in (5.2.6) is effectively a Gaussian white noise term but with a variance dependent on $\phi$, the phase tracking error. This is an intuitive result which follows from the modulation bandwidth greatly exceeding that of $\phi$. This assumption about n"(t) is a necessary one. Otherwise, the problem cannot be solved by Fokker-Planck techniques [17].

In Fig. 21 the VCO phase output follows from combining (5.2.3) and (5.2.8):

$$\hat{\theta} = \frac{K_v}{s} (z_u + z_\ell)$$

$$= \frac{K_v}{s} \{K_1 K_{1m} F_1(s) [(m^2P)^{\frac{1}{2}} \sin \phi + n'(t)]$$

$$+ \frac{1}{2} K_2 K_{2m} F_3(s) \{[(1-m^2)P]^{\frac{1}{2}} A \sin 2\phi + n"(t)\} \qquad (5.2.9)$$

where $K_v$ is the VCO gain. The assumption of a first-order tracking loop will now be applied, i.e., $F_1(s) = F_3(s)$

have unit gains. Hence, using $\hat{\theta} = \theta - \phi$ in (5.2.9), the stochastic differential equation governing loop operation is

$$\dot{\phi} = \Omega_o - \{K_u(m^2P)^{\frac{1}{2}} \sin \phi + \frac{K_\ell}{2} A[1-m^2)P]^{\frac{1}{2}} \sin 2\phi + n_e(t)\} \tag{5.2.10}$$

where $K_u = K_1 K_{1m} K_v$, $K_\ell = K_2 K_{2m} K_v$ are the upper and lower loop gains respectively and $n_e(t)$ is a white noise process with spectral density.

$$S(\omega) \doteq \frac{N_o K_u^2}{2} [1 + 2G^2 (\underline{\sigma}_d^2 \cos^2 \phi + \sigma^2)] \tag{5.2.11}$$

where $G \triangleq K_\ell/K_u$ and $\theta(t) = \Omega_o t + \theta$. The form of $\theta(t)$ represents the sum of a frequency offset term, $\Omega_o t$, and a slowly varying phase angle, $\theta$, which is taken to be uniformly distributed in $[-\pi, \pi]$.

It has been shown in Sec. 4.4 that the steady-state solution to the stochastic equation

$$\dot{\phi} = P(\phi) + \sqrt{G(\phi)}\ \underline{n}(t) \tag{5.2.11}$$

is solved by applying (4.4.4)

$$\frac{d}{d\phi} G(\phi)\ p(\phi) - \frac{4}{N_o} P(\phi)\ p(\phi) = C \tag{5.2.12}$$

Comparing (5.2.10) and (5.2.11) gives

$$P(\phi) = \Omega_o - K_u(m^2P)^{\frac{1}{2}} \sin \phi - \frac{K_\ell}{2} A[1-m^2)P]^{\frac{1}{2}} \sin 2\phi$$

$$G(\phi) = K_u^2 \{1 + 2G^2 [\underline{\sigma}_d^2 \cos^2 \phi + \sigma^2]\} .$$

Using these results in (5.2.12), integrating and invoking the boundary condition $p(\pi) = p(-\pi)$, yields

$$P(\phi) = N \exp[U(\phi)] \tag{5.2.13a}$$

where N is a normalization constant and the potential function $U(\phi)$ is given by

$$U(\phi) = B_1 \tan^{-1}\left[\left(\frac{M}{M+1}\right)^{\frac{1}{2}} \tan\phi\right] + B_2 \tan^{-1}\left[\frac{\cos\phi}{M^{\frac{1}{2}}}\right] + B_3 \ln(M + \cos^2\phi) \tag{5.2.13b}$$

with

$$B_1 = \frac{2\Omega_o}{N_o K_u^2 G^2 \underline{\sigma}_d^2 [M(M+1)]^{\frac{1}{2}}},$$

$$B_2 = \frac{2(m^2 P)^{\frac{1}{2}}}{N_o K_u \underline{\sigma}_d^2 G^2 M^{\frac{1}{2}}},$$

$$B_3 = \frac{K_\ell A[(1-m^2)P]^{\frac{1}{2}} - N_o K_u^2 G^2 \underline{\sigma}_d^2}{\underline{\sigma}_d^2 K_u^2 G^2 N_o},$$

$$M = \frac{1 + 2G^2\sigma^2}{2G^2\underline{\sigma}_d^2}$$

An explanation of the pdf derivation is given in Appendix B.

## 5.3 Loop Parameter Optimization

The optimization procedure discussed here is identical to the method proposed by [11]. The loop SNR of an SPLL with rms signal amplitude $A'$ and gain K is given by [6]:

$$\rho = \frac{4A'}{N_o K} = \frac{2A'^2}{N_o W_L} \tag{5.3.1}$$

where $W_L = A'K/2$ is the double-sided bandwidth and $A' = (m^2 P)^{\frac{1}{2}}$. An effective SNR may be defined for the data-aided carrier tracking loop in its linear region of operation

$$\rho_e = \frac{4A_e}{N_o K_e} = \frac{2A_e^2}{N_o W_{Le}} \tag{5.3.2}$$

where

$$A_e = \frac{A'[1 + GAR]}{[1+2G^2(\sigma_d^2+\sigma^2)]^{\frac{1}{2}}} \tag{5.3.3}$$

is the effective tracking loop rms amplitude given in terms of SPLL parameters and

$$R = [\frac{(1-m^2)}{m^2}]^{\frac{1}{2}} ,$$

$$K_e = K(\frac{K_u}{K}) [1 + 2G^2 (\sigma_d^2 + \sigma^2)]^{\frac{1}{2}} . \tag{5.3.4}$$

Using (5.3.1) - (5.3.4), a maximization ratio may be defined:

$$I \triangleq \frac{\rho_e}{\rho} = \frac{K}{K_u} \frac{(1+GAR)}{[1+2G^2(\sigma_d^2+\sigma^2)]} . \qquad (5.3.5)$$

The data-aided tracking loop and SPLL bandwidths can be compared by

$$\frac{W_{Le}}{W_L} = \frac{K_u}{K} (1+GAR) \qquad (5.3.6)$$

The optimization procedure involves choosing $K_u$ and G such that $\rho_e$ is maximized when $W_{Le}/W_L = 1$. As $\rho_e = 2A_e^2/N_o W_{Le}$, the optimization is equivalent to maximizing $A_e^2$ with respect to G. Differentiation of (5.3.3) squared with respect to G and equating to 0 gives

$$G = G_o$$

$$= \frac{AR}{2(\sigma_d^2+\sigma^2)} . \qquad (5.3.7)$$

Using (5.3.7) in (5.3.6) gives

$$\frac{K}{K_u} = 1 + G_o AR$$

and hence,

$$I_{max} \triangleq \left(\frac{\rho_e}{\rho}\right)_{max} = \frac{(1+G_o AR)^2}{[1+2G_o^2(\sigma_d^2+\sigma^2)]}$$

$$= m^2 S \qquad (5.3.8)$$

where

$$S = \frac{A^2}{2(\underline{\sigma}_d^2+\sigma^2)} + m^2 \left[1 - \frac{A^2}{2(\underline{\sigma}_d^2+\sigma^2)}\right] .$$

Solving for $K_u$ and $K_\ell$ yields

$$K_u = \frac{m^2 K}{S} , \quad K_\ell = \frac{m^2 ARK}{S} \tag{5.3.9}$$

Substitution of $G_o$ in (5.2.13b) yields for the potential function

$$U(\phi) = \frac{2\Omega_o}{K_{oo}} \tan^{-1}\left[\left(\frac{M}{M+1}\right)^{\frac{1}{2}} \tan\phi\right] + \frac{\rho}{2} \frac{(1+G_o AR)}{\underline{\sigma}_d^2 G_o^2} \cdot$$

$$\left\{\frac{1}{M^{\frac{1}{2}}} \tan^{-1}\left(\frac{\cos\phi}{M^{\frac{1}{2}}}\right) + \frac{1}{2}\left[AG_o R - \frac{2\,\underline{\sigma}_d^2 G_o^2}{\rho(1+G_o AR)}\right] \cdot \right.$$

$$\left. \ln(M + \cos^2\phi)\right\} \tag{5.3.10}$$

where

$$K_{oo} = \{N_o K_u^2 G_o^2 \underline{\sigma}_d^2 [M(M+1)]^{\frac{1}{2}}\}^{-1}$$

Equation (5.3.10) gives the phase pdf potential function in terms of the SNR of an SPLL with the same bandwidth as the data-aided carrier tracking loop.

## 5.4 Results

The results presented here are applicable to two data communication channels. The first channel - Channel 1 - has been described in Sec. 3.5. Briefly,

the channel has a low pass impulse response $h_c(t) = ae^{-at}$ and p(t), the input pulse waveform, is rectangular and of width T. The weight $\psi_i$ and filtered white noise variance $\sigma^2$ required to evaluate the error rate bounds described in Sec. 3.4 are taken from equations (9), (14), (31) and (32) of [4]. The values applicable when the equalizer SNR = 16 dB have been given in Sec. 3.7.

The results for the coherent receiver - here, the data-aided carrier tracking loop - are presented in Fig. 22. The phase, $\theta$, is uniformly distributed on $[-\pi, \pi]$ and thus it is clear from Figs. 14 and 8 of Chap. 3 that the system error rate would be unacceptable for the zero phase receiver. In Fig. 22 the average of the upper and lower bounds is plotted as a function of modulation index m with the ratio of equalizer bandwidth to tracking loop bandwidth as a parameter. Here, as with all the results pertaining to the data-aided loop, the "no-detuning case" [11] will be treated, i.e., $\dot{\theta} = \Omega_o = 0$. Equation (5.3.10) gives the error phase pdf as a function of m and $\rho$ where $\rho$ is the SNR of an SPLL having the same bandwidth as the data-aided loop. As the signal presented to the equalizer is the same regardless of whether the SPLL or data-aided loop is used, then (4.5.6) can be used in (5.3.10). As $\rho$ in (4.5.6) is a function of m and $\phi/B$, so must also $p(\phi)$ be dependent upon these variables. The upper and lower

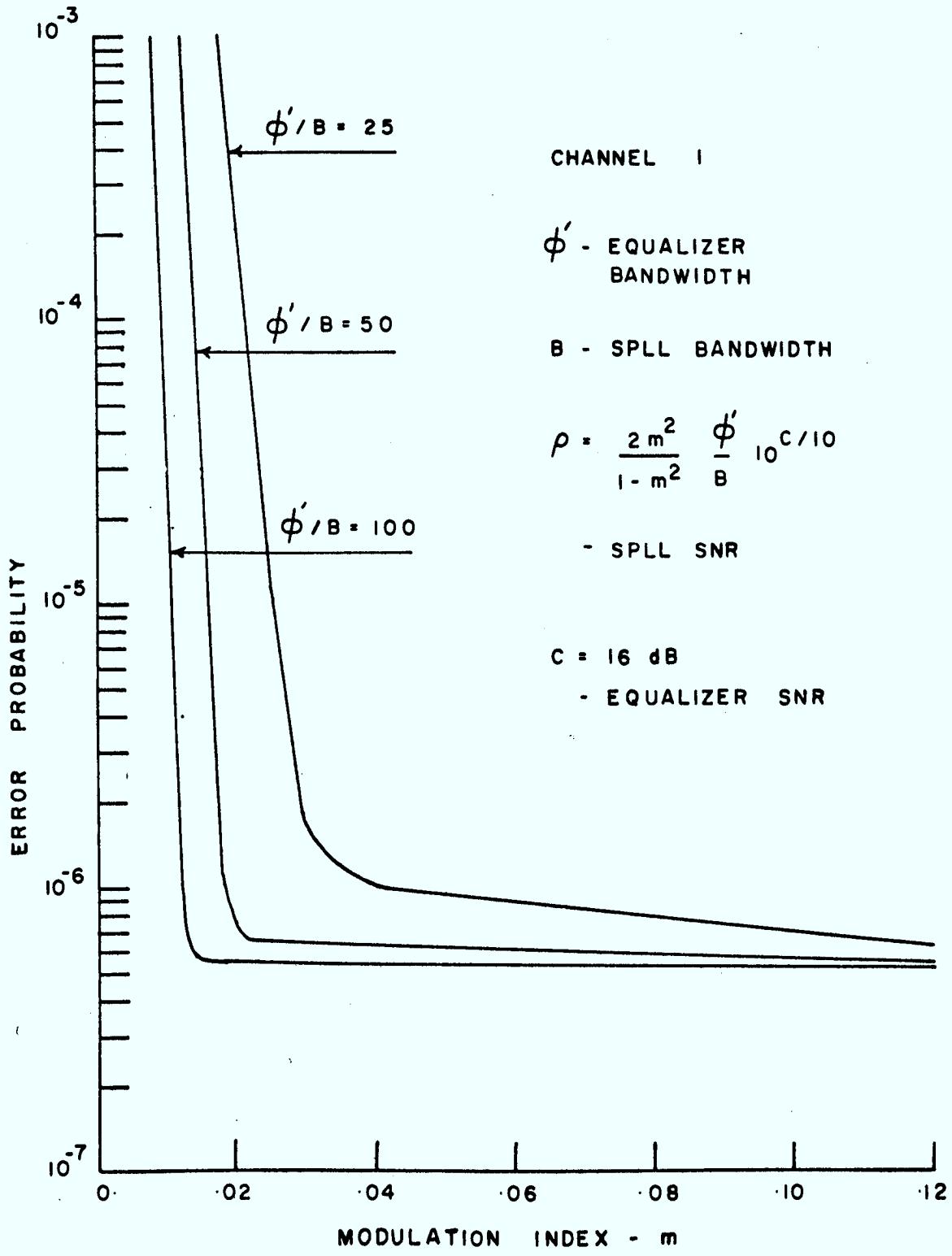


FIGURE 22: ERROR RATE VERSUS MODULATION INDEX WITH DATA-AIDED TRACKING LOOP IN RECEIVER - CHANNEL 1

bounds were found to agree to within a factor of 7 indicating that the arithmetic average of these bounds represents a plausible estimate of P(error). It is seen that the system is useful when $m > .02$. For $m < .02$, a threshold phenomenon occurs and performance degrades dramatically. From Figure 19, the threshold for the standard phaseback loop and $\phi'/B = 50$ is $m = .12$. Thus, the data aided loop requires 6 dB less power to operate at the nominal error rate.

The results given in Fig. 23 apply to Channel 2, with SNR = 13 dB, which was reviewed in Sec. 3.10. The bounds for this channel were found to differ by, at most, a factor of 7. The average of the upper and lower bounds is plotted in Fig. 23 for the same parameters as in Fig. 22. Again, the threshold phenomenon for small m is evident and this is to be compared with the monotone degradation curves of Fig. 20.

This threshold performance is caused by a phase ambiguity arising at $\pm \pi$ radians as $m \to 0$. Rather than being monotone decreasing from 0 to $\pi$ (and from 0 to $-\pi$) as occurs with the SPLL, the phase pdf decays from 0 to some value $\theta$, but then becomes significant near $\pi$ radians. As the error bounds are very large for large $\theta$, integration over a pdf with a significant value about $\pi$ will result in an unacceptable error rate. When $m = 0$ the upper loop of the data-aided loop is inoperative. This means that the first term in (5.2.9) should be equated to zero. Following the procedure of Sec. 5.2 the potential function is of the form

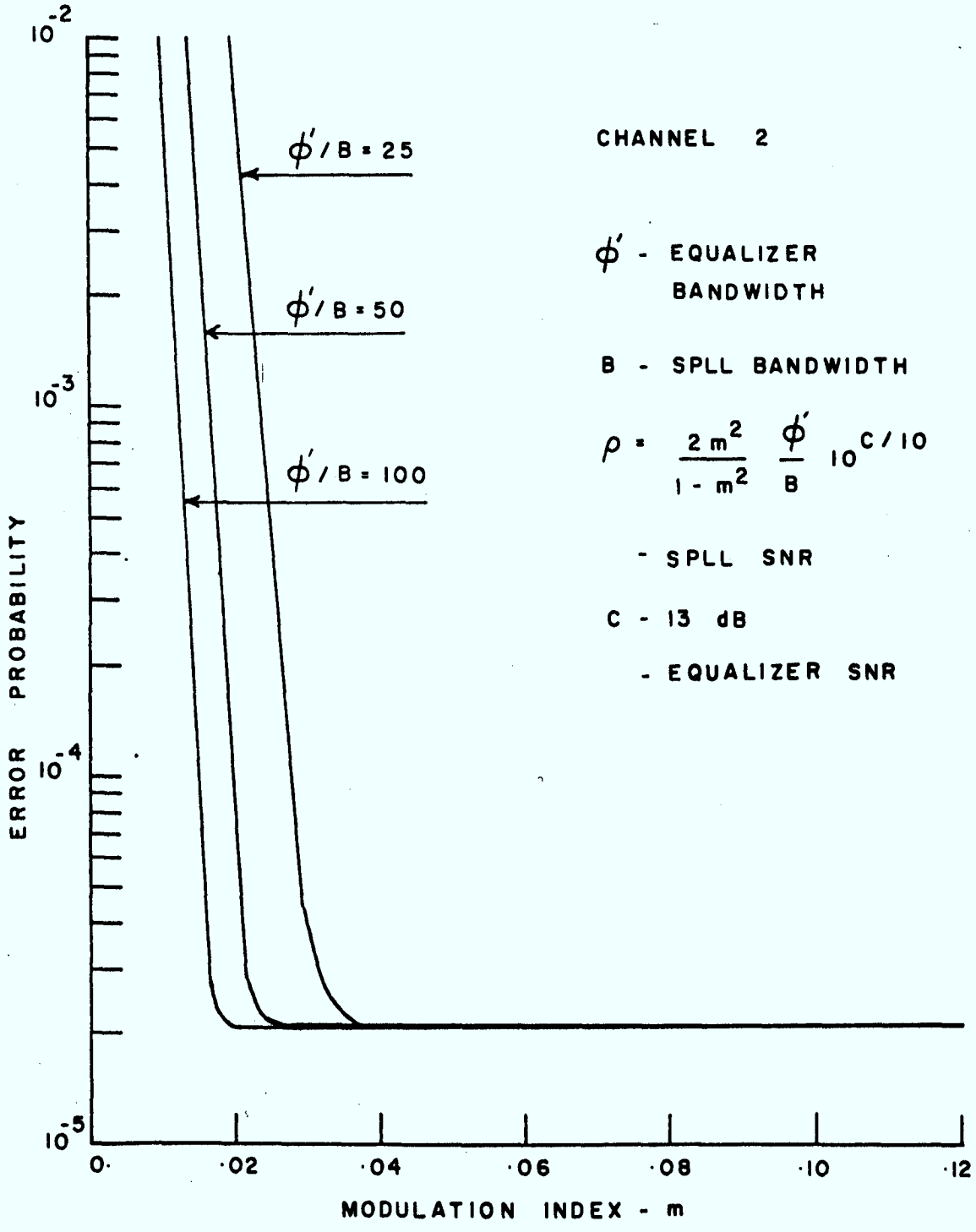


FIGURE 23: ERROR RATE VERSUS MODULATION INDEX WITH DATA-AIDED TRACKING LOOP IN RECEIVER - CHANNEL 2

$$U(\phi) = C_1 \ln(M+\cos^2 \phi) \qquad (5.4.1)$$

where $C_1$ is a constant and $U(\phi)$ is periodic with period $\pi$. For (5.4.1) above, $p(\pm\pi) = p(o)$ and a phase ambiguity occurs. Thus, the system P(error) exceeds 0.5 and performance is completely unacceptable. The ambiguity phenomenon also occurs in the non-intersymbol interference case (see Figs. 9 and 15 of [11]).

## 5.5 Summary

A phase coherent receiver incorporating a data-aided carrier tracking loop for phase tracking purposes and an equalizer for estimation of the baseband signal has been examined. Previously, the tracking loop had been analyzed only for a non-bandlimited channel. Beyond threshold it was found that the tracking loop effectively compensates for carrier phase jitter by restraining the error rate to within a region of the nominal, zero-phase error probability. The receiver structure requires that a reference carrier be transmitted with the modulation. While the absence of the carrier means greater power possible in the modulation the resulting loop phase output exhibits an unacceptable pdf ambiguity. Hence, if suppressed carrier operation is desired another receiver must be considered.

# CHAPTER 6

# CONCLUSIONS

Here, the contributions of this report are reviewed. Suggestions for future work are given.

## 6.1 Summary

The emphasis of this report has been placed upon the study of carrier phase jitter effects upon receiver performance for PAM transmission. The problem of phase jitter is a real one. For example, it appears in spacecraft communications [11] and over long-haul switched telephone lines [18]. In examining the phase jitter phenomenon this report has made the following contributions:

1) The degradation in performance of a standard PAM receiver, measured by P(error), was assessed for small values of random phase.
2) Documented bounds on P(error) [4], applicable when the phase lies in the interval $[-\pi/2, \pi/2]$, were extended to include phase values on $[-\pi, \pi]$.
3) Receiver performance when an SPLL is used with the standard baseband receiver was assessed for random phase values in $[-\pi, \pi]$.

4) The data-aided carrier tracking loop was applied to equalized PAM transmission and the receiver performance was analyzed. By including the presence of intersymbol interference in the modulation, the analysis represents an extension of existing theory.

A chapter-by-chapter review of the thesis follows.

In Chapter 2, an expression for the response of a band-restrictive channel was derived for a digital PAM input. It was assumed that in addition to introducing intersymbol interference, the channel also introduced a random phase into the carrier. The channel filter output was distorted by additive Gaussian noise.

Chapter 3 discussed the zero phase receiver. It was found that while small random phase distributions were tolerable, the assumption of a phase uniform on $[-\pi, \pi]$ implied, by the extended bounds on P(error), that receiver performance becomes unacceptable. Hence, for the zero-phase receiver to be useful, the random phase cannot have large values.

In Chapter 4 a standard phase-locked loop was used in the receiver structure to track the random phase in the carrier. Results indicated that proper choice of modulation index could compensate for the phase distortion. However, adjusting for phase jitter reduces transmission efficiency as additional bandwidth is required

for phase referencing.

Chapter 5 discussed the data-aided carrier tracking loop as an improvement upon the SPLL in terms of loop SNR. It was shown that for modulation indices greater than a threshold value, that this type of loop is extremely efficient in removing the error rate degradation due to carrier phase jitter. The data-aided loop has been analyzed previously. However, the solution acknowledging the existence of intersymbol interference represents an extension of the theory given by Lindsey and Simon.

Both the SPLL and data-aided loop make use of a reference carrier. For acceptable tracking, the reference and modulation must be sufficiently separated so as to prevent mutual interference. This condition indicates that this system, using 2-level PAM, may not be practical for telephone line transmission because of the low signalling rate permissible. However, there do exist modems which transmit modulation with reference carriers over telephone lines. For example, the ESE 48/QM Modem Series [19] uses quadrature amplitude modulation with a bandwidth from 1200 Hz to 2400 Hz and pilot carriers at .8 and 2.8 KHz. Another requirement of the systems discussed is that the loop filters must have cut-off points which ensure loop operation as described in Chaps. 4 and 5.

## 6.2 Suggestions for Future Work

Of the assumptions used in this report, probably the most important was that of a conjugate symmetric channel. This does not represent the general situation. In Appendix A, it is shown that when the conjugate component of the channel impulse response is significant, i.e., $h_s(t) \neq 0$, that a quadrature term need be added to the channel output of (2.3.4). Of course, the presence of this term means that the receivers postulated in this text must be modified.

The application of the baseband equalizer PAM receiver was based on correct symbol synchronization. An interesting area for further study would be consideration of timing jitter effects caused by the equalizer sampler. A receiver and its analysis for this problem would be a welcome contribution to the field.

This report has been of a theoretic nature. That is, the error probabilities are based on bounds rather than on simulation or experimental verification. In addition, the operation of the loops, both SPLL and data-aided carrier tracking loop, have been examined on the basis of steady-state operation. The problems associated with acquisition and transient problems have not been examined. The loop results predicted by the theoretical approach have not been checked experimentally.

The analysis given here has assumed the signal to be a double-sideband waveform. The DSB signal is wasteful of bandwidth. Examination of receiver performance when single-sideband modulation (SSB) is transmitted would be very useful for practical communication.

While distortion of the modulation by intersymbol interference has been included in this study, other effects could also be considered. For example, the effect of system non-linearities such as envelope limiters could be investigated.

Finally, a method whereby suppressed carrier operation is feasible would increase the available bandwidth for the modulation. It has been shown that the data-aided loop as described here would be completely unacceptable were the reference signal suppressed.

REFERENCES


1. Carlson, A.B.: Communication Systems. McGraw-Hill (1968)

2. Lucky, R.W., Salz, J. and Weldon, E.J.: Principles of Data Communication. McGraw-Hill (1968)

3. George, D.A., Coll, D.C., Kaye, A.R., Bowen, R.R.: Channel Equalization for Data Transmission. The Engineering Journal, 53, 20 (1970)

4. McLane, P.J.: Error Analysis of Equalizers for Digital Transmission by PAM. Research Report No. 71-2, Department of Electrical Engineering, Queen's University, Kingston (1971)

5. Lugannani, R.: Intersymbol Interference and Probability of Error in Digital Systems. IEEE Trans. Inform. Theory, IT-15, 682 (1969)

6. Ho, E.Y. and Spaulding, D.A.: Data Transmission Performance in the Presence of Carrier Phase Jitter and Gaussian Noise. BSTJ, 51-8, 1927 (1972)

7. Viterbi, A.J.: Principles of Coherent Communication. McGraw-Hill (1966)

8. Gardner, F.M.: Phase Lock Techniques. John Wiley (1966)

9. Lindsey, W.C.: Synchronization Systems in Communications and Control. Prentice-Hall (1972)

10. Stiffler, J.J.: Theory of Synchronous Communications. Prentice-Hall (1971)

11. Lindsey, W.C. and Simon, M.K.: Data-Aided Carrier Tracking Loops. IEEE Trans. Commun. Tech., COM-19, No. 2, 157 (1971)

12. Van Trees, H.L.: Detection, Estimation and Modulation Theory, Part III, John Wiley (1968a)

13. Falconer, D.D. and Gitlin, R.D.: Bounds on Error-Pattern Probabilities for Digital Communications Systems. IEEE Trans. Commun., COM-20, 132 (1972)

14. Van Trees, H.L.: Detection, Estimation, and Modulation Theory, Part II, John Wiley (1968b)

15. Martin, J.: Telecommunications and the Computer. Prentice-Hall (1969)

16. Viterbi, A.J.: Phase-Locked Loop Dynamics in the Presence of Noise by Fokker-Planck Techniques. Proc. IEEE, 51, 1737 (1963)

17. Lindsey, W.C. and Simon, M.K.: Private correspondence.

18. Puchkoff, S.J.: A Modern Eye-Pattern Looks at Telephone Lines. Telecommunications, 6, 20 (1972)

19. ESE Limited: 48/QM Modem Series, B5-72

# APPENDIX A

## A.1 General Channel Response to PAM Input

When the channel is not conjugate symmetric, the channel impulse response is given by

$$h(t) = 2h_c(t) \cos \omega_c t + 2h_s(t) \sin \omega_c t$$

and hence the complex impulse response is

$$\tilde{h}(t) = h_c(t) - j\, h_s(t)$$

where $h_c(t)$ and $h_s(t)$ are defined in Sec. 2.3. Substituting $\tilde{h}(t)$ in (2.3.3) and neglecting double frequency terms, the filter output becomes

$$z(t) = \sqrt{2} \sum_{n=0}^{N-1} \xi_n \int_0^t \mathrm{Re}[\tilde{h}(t-\tau)\, p(\tau-nT)\, e^{j(\omega_c t+\theta)}]d\tau$$

$$= \sqrt{2} \sum_{n=0}^{N-1} \xi_n\, g_1(t-nT) \cos(\omega_c t+\theta)$$

$$+ \sqrt{2} \sum_{n=0}^{N-1} \xi_n\, g_2(t-nT) \sin(\omega_c t+\theta) \qquad \text{(A.1.1)}$$

where

$$g_1(t) = \int_0^t h_c(t-\tau)\, p(\tau)d\tau$$

$$= h_c(t) \circ p(t) \ ,$$

$$g_2(t) = \int_0^t h_s(t-\tau)\ p(\tau)d\tau$$

$$= h_s(t) \circ p(t)$$

and $\circ$ denotes causal convolution.

# APPENDIX B

## B.1 Derivation of Phase PDF

Here, a clarification of the derivation of the phase pdf is given.

In Sec. 5.2 it was shown that $p(\phi)$ could be obtained by solving

$$\frac{d}{d\phi} G(\phi)\, p(\phi) - \frac{4}{N_o} P(\phi)\, p(\phi) = C \qquad \text{(B.1.1)}$$

with

$$P(\phi) = \Omega_o - K_u(m^2P)^{\frac{1}{2}} \sin\phi - \frac{K_\ell}{2} A[(1-m^2)P]^{\frac{1}{2}} \sin 2\phi$$

$$G(\phi) = K_u^2\{1+2G^2\,[\underline{\sigma}_d^{\,2} \cos^2\phi + \sigma^2]\}$$

Substitution of $P(\phi)$ and $G(\phi)$ in (B.1.1) and expanding (B.1.1) gives

$$\frac{d\,p(\phi)}{d\phi} + \frac{4}{N_o K_u^2}\{-\Omega_o + K_u(m^2P)^{\frac{1}{2}} \sin\phi \cdot$$

$$+ [\frac{K_\ell A}{2}\,[(1-m^2)P]^{\frac{1}{2}} - \frac{N_o K_u^2\, \underline{\sigma}_d^{\,2} G^2}{2}] \sin 2\phi\}$$

$$[1 + 2G^2\,(\underline{\sigma}_d^{\,2} \cos^2\phi + \sigma^2)]^{-1}\, p(\phi)$$

$$= \frac{4C_1}{N_o K_u^2[1+2G^2(\underline{\sigma}_d^{\,2}\cos^2\phi+\sigma^2)]} \qquad \text{(B.1.2)}$$

Equation (B.1.2) is of the form

$$\frac{dy}{dx} + R(x)y = Q(x) \qquad \text{(B.1.3)}$$

whose solution is

$$y(x) = [\mu(x)]^{-1} \left[\int^{x} \mu(s)\, Q(s)\, ds + C_2\right] \qquad \text{(B.1.4a)}$$

where

$$[\mu(x)]^{-1} = \exp\left[-\int^{x} R(t)\, dt\right] \qquad \text{(B.1.4b)}$$

Let

$$U(\phi) = -\int^{\phi} R(t)\, dt \qquad \text{(B.1.5)}$$

Comparing (B.1.2) and (B.1.3) gives for $U(\phi)$

$$U(\phi) = \frac{2\Omega_o}{N_o K_u^{\,2} G^2 \underline{\sigma}_d^{\,2}} \int^{\phi} \frac{dt}{M+\cos^2 t} - \frac{2(m^2 P)^{\frac{1}{2}}}{N_o K_u G^2 \underline{\sigma}_d^{\,2}} \int^{\phi} \frac{\sin t\, dt}{M+\cos^2 t}$$

$$- \frac{[K_\ell A[(1-m^2)P]^{\frac{1}{2}} - N_o K_u^{\,2} G^2 \underline{\sigma}_d^{\,2}}{N_o K_u^{\,2} G^2 \underline{\sigma}_d^{\,2}} \int^{\phi} \frac{\sin 2t\, dt}{M+\cos^2 t} \qquad \text{(B.1.6)}$$

Integrating the terms of (B.1.6) gives the result of (5.2.13b). Using (B.1.4a) the phase pdf is given by

$$p(\phi) = \exp[U(\phi)]\left[\int_{-\pi}^{\phi} \exp[-U(s)]\, Q(s)\, ds + C_2\right]$$

$$= N \exp[U(\phi)]\left[D \int_{-\pi}^{\phi} \exp[-U(s)]\, Q(s)\, ds + 1\right] \qquad \text{(B.1.7)}$$

Using the boundary condition $p(\pi) = p(-\pi)$ and noting that $U(\pi) = U(-\pi)$ gives

$$p(\phi) = N \exp[U(\phi)] \qquad \text{(B.1.8)}$$

where N is a normalization constant.

MATYAS, ROBERT
--Error analysis of digital communication by PAM on equalized, band restricted and incoherent channels